High accuracy mixed finite element-differential quadrature method for free vibration of axially moving orthotropic plates loaded by linearly varying in-plane stresses

S. A. Eftekhari1[a,*], A. A. Jafari[b]

[a]*Young Researchers and Elite Club, Karaj Branch, Islamic Azad University, Karaj, P.O. Box 31485-313, Iran*

[b]*Mechanical Engineering Department, K. N. Toosi University of Technology, Tehran, P.O. Box 19395-1999, Iran*

Abstract

A high order accurate mixed finite element-differential quadrature method is proposed to study the dynamics of axially moving orthotropic rectangular plates subjected to linearly varying inplane stresses. The finite element method (FEM) with higher order interpolation functions is first used to discretize the spatial partial derivatives with respect to a co-ordinate direction of the plate. The differential quadrature method (DQM) is then employed to discretize the resulting system of ordinary differential equations. Linearly varying uniform and non-uniform distributed load conditions are considered on two-opposite edges of the plate. Comparisons are made with existing numerical and analytical solutions in the literature. It is revealed that the proposed mixed method is highly accurate and efficient. Finally, the dimensionless complex frequencies of the axially moving orthotropic plate with different boundary conditions under the linearly varying inplane stresses are calculated by the proposed mixed method. The curves for the real and imaginary parts of the first three dimensionless complex frequencies versus the dimensionless axially moving speed are obtained. The effects of material properties of the plate, variation of inplane stresses, and the dimensionless moving speed on the stability of the orthotropic plate are investigated.

***Keywords*:** FEM; DQM; Higher order interpolation functions; Axially moving orthotropic plates; Linearly varying inplane stresses; Divergence and flutter instabilities.

1. Introduction

The dynamic behavior of axially moving plate-like structures is of great interest for a variety of engineering applications. In the aerospace engineering field for instance, the behavior of aircraft wings can be modeled using this approach. Other important applications include, but are not limited to, band saw blades, conveyor belts and chain in power transmission lines, and the steel strip in a thin steel sheet production. Many researchers have shown that the axial moving speed plays important roles on the vibration characteristics and dynamics of such systems. An interesting manifestation of

[*] Corresponding author. Tel.: +98 9194618599; Fax: +98 26 34418156.
E-mail address: aboozar.eftekhari@gmail.com (S. A. Eftekhari)

this subject is that when the structure is moving at high-speeds, a critical velocity is found existing, which may cause a significant vibration of the structure response. Thus, it is important to accurately predict the dynamic behavior and vibration characteristics of axially moving plates for the successful design and safe operation of such structures.

The string and beam theories are two popular ones that are widely used by many researchers to model the problem and to investigate the dynamics of axially moving systems [1-9]. Although these simple models may lead to reasonable and satisfactory results for some special cases, they cannot correctly describe the two-dimensional behavior of moving structures. Therefore, many researchers have employed the plate model to examine the dynamic behavior of such structures [10-19]. However, most studies on moving plate problem involved either isotropic plates or moving plates subjected to uniform tension. Such idealizations are not quite true because most structures that are moving axially are orthotropic in nature and influences of non-uniform inplane loading cannot be ignored in the analysis of such structures. On the other hand, to the authors' best knowledge, the information regarding the free vibration of axially moving *multi-span* orthotropic plates *subjected to linearly varying in-plane stresses* is rare and this is the reason why this paper tries to study the title problem.

Two kinds of methods, i.e., analytical and numerical methods have been widely used over past few decades to tackle the problem. As analytical methods are often limited to simple moving beam or plate problems, many researchers have resorted to various numerical methods. The finite element method (FEM) is one of the most versatile numerical methods used by many researchers to handle the problem. Although the FEM is especially powerful due to its versatility in the spatial discretization, the number of unknowns involved and the amount of input data are very large in FEM. To overcome this difficulty, higher order methods can be employed. Among them, the differential quadrature method [20-23], the Kantorovich method [24], the discrete singular convolution (DSC) method [25, 26], the differential transform method [27] and recently the differential quadrature finite element method [28, 29] have been successfully applied to various plate problems.

Alternatively, in a series of papers, the present authors proposed a number of mixed methodologies where the number of unknowns is substantially reduced [30-33]. In these mixed methods, the Ritz method or the FEM is first employed to discretize the spatial partial derivatives with respect to a co-ordinate direction of the plate. The differential quadrature method (DQM) is then used to discretize the resulting system of ordinary differential equations. The proposed mixed methods were claimed to enjoy the advantages of both component methods and overcome some limitations of each component method. Although highly accurate solutions were obtained using the mixed Ritz-DQM [30, 31] and mixed DQ-Ritz method [32] for vibration and buckling problems of rectangular plates, the application of these methods are limited to the plate problems where the geometry and material properties do not vary along two co-ordinate directions (due to the use of continuous smooth functions in both co-ordinate directions of the plate). This limitation can be overcome by using the mixed FE-DQM [33]. Due to the use of piecewise discontinuous functions in on co-ordinate direction of the plate, the method can easily handle the plate problems with varying geometry, material properties, and loading in that direction.

The capability of the mixed FE-DQM for free and forced vibration, and buckling analysis of rectangular plates was well studied in Ref. [33]. Although the method was shown to work well for the problems considered, the accuracy and convergence rates were not very satisfactory due to the use of Hermite interpolation functions in the mixed method. In fact, the accuracy and convergence rates of the numerical mixed method were more significantly influenced by the relative low accuracy of the FEM and could not explain higher accuracy of the mixed FE-DQM. To tackle the above-mentioned difficulties, this paper presents a high order accurate mixed FE-DQM in which the accuracy and convergence rates are significantly improved. The proposed mixed method uses the FEM with higher order interpolation functions in one co-ordinate direction of the plate and the DQM in other one. Thus, the accuracy and convergence rates can be easily improved by increasing the order of FEM interpolation functions. Its stability, rate of convergence, and accuracy are challenged through the solution of some benchmark vibration and buckling problems. It is shown that by using the higher order interpolation functions in the mixed FE-DQ formulation, highly accurate solutions can be achieved using a small number of finite elements (in most cases using only *one finite element*). This requires less computational effort compared to the formulation presented in Ref. [33] where cubic interpolation functions were employed in one co-ordinate direction of the plate.

2. Governing equation and FEM formulation

The physical system analyzed is an elastic orthotropic rectangular plate of N spans with thickness h, length a, width b, mass density ρ, subjected to initial stresses due to a non-uniform edge force N_x, and moving with a constant speed v along x-direction, as shown in Fig. 1. The plate is assumed to be orthotropic with the principal material direction coinciding with the x and y axes ($0 \le x, y \le a, b$). The governing differential equation for the motion of the axially moving orthotropic plate based on the Love-Kirchhoff theory is

$$D_{11}w_{,xxxx} + 2D_{33}w_{,xxyy} + D_{22}w_{,yyyy} + \rho h\left(w_{,tt} + 2vw_{,xt} + v^2 w_{,xx}\right) = N_x w_{,xx} \tag{1}$$

where a subscript comma denotes differentiation, w is the transverse displacement of the plate, and

$$D_{11} = \frac{E_1 h^3}{12(1-\mu_{12}\mu_{21})}, \qquad D_{22} = \frac{E_2 h^3}{12(1-\mu_{12}\mu_{21})}, \quad D_{33} = D_{12} + 2D_{66}$$

$$D_{12} = \mu_{12}D_{22} = \mu_{21}D_{11}, \qquad D_{66} = \frac{G_{12}h^3}{12} \tag{2}$$

where the expressions for D_{11}, D_{22}, D_{12} and D_{66} represent the flexural rigidities and the torsional rigidity of the orthotropic plate, respectively. Moreover, E_1, E_2, and G_{12} are orthotropic plate moduli, and μ_{12} and μ_{21} are Poisson ratios.

In this study, the inplane force N_x is assumed to be linear function of y (i.e., $N_x = N_x(y)$). For convenience, let $N_x = N_0 f(y) = N_0 |1-\alpha \frac{y}{b}|$, where α is a parameter that defines the relative tension. Fig. 2 shows a rectangular plate under different types of edge loading. The boundary conditions of the orthotropic plate are

(I) Simply-supported edge (S)

$$w = D_{11}w_{,xx} + D_{12}w_{,yy} = 0 \quad \text{at} \quad x = 0 \text{ or } a \tag{3}$$

$$w = D_{22}w_{,yy} + D_{12}w_{,xx} = 0 \quad \text{at} \quad y = 0 \text{ or } b \tag{4}$$

(II) Clamped edge (C)

$$w = w_{,x} = 0 \quad \text{at} \quad x = 0 \text{ or } a \tag{5}$$

$$w = w_{,y} = 0 \quad \text{at} \quad y = 0 \text{ or } b \tag{6}$$

(III) Free edge (F)

$$D_{11}w_{,xx} + D_{12}w_{,yy} = D_{11}w_{,xxx} + (2D_{33} - D_{12})w_{,xyy} = 0 \quad \text{at} \quad x = 0 \text{ or } a \tag{7}$$

$$D_{22}w_{,yy} + D_{12}w_{,xx} = D_{22}w_{,yyy} + (2D_{33} - D_{12})w_{,yxx} = 0 \quad \text{at} \quad y = 0 \text{ or } b \tag{8}$$

It is convenient to introduce the following dimensionless parameters and variables:

$$\bar{x} = x/a,\ \bar{y} = y/b,\ \overline{D}_{11} = D_{11}/D_{33},\ \overline{D}_{22} = D_{22}/D_{33}, \bar{v} = va.\left(\frac{\rho h}{D_{33}}\right)^{1/2},\ \bar{t} = \frac{t}{a^2}\left(\frac{D_{33}}{\rho h}\right)^{1/2},$$

$$\overline{N}_x = N_x a^2/D_{33},\ \lambda = a/b \tag{9}$$

where $\bar{t}$ is the non-dimensional time. Substituting above dimensionless parameters and variables into governing equation of motion of the axially moving orthotropic plate yields

$$D_{11}w_{,xxxx} + 2\lambda^2 w_{,xxyy} + \lambda^4 D_{22}w_{,yyyy} + w_{,tt} + 2vw_{,xt} + v^2 w_{,xx} = N_x w_{,xx},\ N_x = N_0 f(y) = N_0 |1-\alpha y| \tag{10}$$

where the over bar of the symbols are omitted for simplicity in notations while causing no confusion.

The free vibration response of the moving orthotropic rectangular plate can be expressed as

$$w(x,y,t) = W(x,y)\exp(\Omega t) \tag{11}$$

Substituting Eq. (11) into Eq. (10) gives

$$D_{11}W_{,xxxx} + 2\lambda^2 W_{,xxyy} + \lambda^4 D_{22}W_{,yyyy} + \Omega^2 W + 2v\Omega W_{,x} + v^2 W_{,xx} = N_x W_{,xx} \tag{12}$$

The domain of the problem along the *x*-axis is first discretized into *n* number of finite elements. The polynomial approximation of the solution within a typical finite element is then assumed as

$$W^e(x,y) = c_1(y) + c_2(y)\bar{x} + c_3(y)\bar{x}^2 + ... + c_{p+1}(y)\bar{x}^p = \sum_{j=1}^{p+1} c_j(y)\bar{x}^{j-1} \quad , \ \bar{x} = x - x_e \tag{13}$$

where $\bar{x}$ is the local co-ordinate of the *e*th finite element with origin fixed at the left end of the element, x_e is the global co-ordinate of the first node of the *e*th finite element, *p* is the order of interpolation functions, and $c_1, c_2, c_3, ..., c_{p+1}$ are unknown coefficients (that are functions of *y*). To ensure the continuity conditions between adjacent elements, these coefficients should be expressed in terms of the displacement parameters. Let the (*p*+1)-parameter polynomial, given in Eq. (13), ensures only the compatibility of deflection and transverse slope at element boundaries (i.e., each node is assumed to have only two degrees of freedom). Thus, the local co-ordinates of the element nodes become $\bar{x}_1, \bar{x}_2, \bar{x}_3, ..., \bar{x}_{(p+1)/2}$ (Note that, in this case, the order of interpolation functions (*p*) must be an odd number, i.e., $p = 3,5,7,9,...$). Now, satisfying the essential boundary conditions of the element (deflections and transverse slopes at the nodes) gives

$$\begin{Bmatrix} W_1^e \\ W_2^e \\ W_3^e \\ W_4^e \\ . \\ . \\ . \\ W_p^e \\ W_{p+1}^e \end{Bmatrix} = \begin{bmatrix} 1 & \bar{x}_1 & \bar{x}_1^2 & \bar{x}_1^3 & . & . & . & \bar{x}_1^{p-1} & \bar{x}_1^p \\ 0 & 1 & 2\bar{x}_1 & 3\bar{x}_1^2 & . & . & . & (p-1)\bar{x}_1^{p-2} & px_1^{p-1} \\ 1 & \bar{x}_2 & \bar{x}_2^2 & \bar{x}_2^3 & . & . & . & \bar{x}_2^{p-1} & \bar{x}_2^p \\ 0 & 1 & 2\bar{x}_2 & 3\bar{x}_2^2 & . & . & . & (p-1)x_2^{p-2} & p\bar{x}_2^{p-1} \\ . & . & . & . & . & . & . & . & . \\ . & . & . & . & . & . & . & . & . \\ . & . & . & . & . & . & . & . & . \\ 1 & \bar{x}_{(p+1)/2} & \bar{x}_{(p+1)/2}^2 & \bar{x}_{(p+1)/2}^3 & . & . & . & \bar{x}_{(p+1)/2}^{p-1} & \bar{x}_{(p+1)/2}^p \\ 0 & 1 & 2\bar{x}_{(p+1)/2} & 3\bar{x}_{(p+1)/2}^2 & . & . & . & (p-1)\bar{x}_{(p+1)/2}^{p-2} & p\bar{x}_{(p+1)/2}^{p-1} \end{bmatrix} \begin{Bmatrix} c_1 \\ c_2 \\ c_3 \\ c_4 \\ . \\ . \\ . \\ c_p \\ c_{p+1} \end{Bmatrix} \tag{14}$$

or

$$\{W^e\} = [X]\{c\} \tag{15}$$

Inverting this matrix equation to express c_i ($i = 1,2,..., p+1$) in terms of nodal displacements W_i^e ($i = 1,2,..., p+1$), and substituting the result into Eq. (13), one obtains

$$W^e(x,y) = \sum_{j=1}^{p+1} W_j^e(y)\phi_j^e(x) \tag{16}$$

where $W_j^e(y)$ are nodal values of the *e*th finite element, and $\phi_j^e(x)$ are the interpolation functions of degree *p*.

Now, substitution of Eq. (16) into Eq. (12), multiplying both sides of resulting equation by $\phi_i^e(x)$, and performing the integration over the length of the *e*th finite element ($x_e \le x \le x_{e+1}$), we obtain

$$D_{11}[A^e]\{W^e\} + 2\lambda^2[C^e]\{W^e_{,yy}\} + \lambda^4 D_{22}[B^e]\{W^e_{,yyyy}\} + \Omega^2[B^e]\{W^e\} + 2v\Omega[D^e]\{W^e\} + v^2[C^e]\{W^e\} = N_x[C^e]\{W^e\} \tag{17}$$

where

$$A^e_{ij} = \int_{x_e}^{x_{e+1}} \phi^e_{i,xx}\phi^e_{j,xx}\mathrm{d}x + [\phi^e_i\phi^e_{j,xxx} - \phi^e_{i,x}\phi^e_{j,xx}]_{x_e}^{x_{e+1}},\ B^e_{ij} = \int_{x_e}^{x_{e+1}} \phi^e_i\phi^e_j\mathrm{d}x,\ C^e_{ij} = -\int_{x_e}^{x_{e+1}} \phi^e_{i,x}\phi^e_{j,x}\mathrm{d}x + [\phi^e_i\phi^e_{j,x}]_{x_e}^{x_{e+1}}$$

$$D^e_{ij} = \int_{x_e}^{x_{e+1}} \phi^e_i\phi^e_{j,x}\mathrm{d}x\ ,\ \ i, j = 1,2,..., p+1 \tag{18}$$

It is noted that the elements of the above matrices can be exactly computed without any difficulty; however, for large values of *p*, it is better to use the integral quadrature rule to reduce the computational time.

The assembly of finite element equations (17) and implementation of boundary conditions are similar to those of one-dimensional beam element equations (see Ref. [34] for detail). By doing so, we obtain the following assembled equation

$$D_{11}[A]\{W\} + 2\lambda^2[C]\{W_{,yy}\} + \lambda^4 D_{22}[B]\{W_{,yyyy}\} + \Omega^2[B]\{W\} + 2v\Omega[D]\{W\} + v^2[C]\{W\} = N_x[C]\{W\} \tag{19}$$

Mathematically, Eq. (19) represents a system of linear coupled ordinary differential equations of fourth-order. In this study, the system (19) will be reduced to a set of algebraic equations by the application of the DQ method.

3. DQ analogues of resulting system of ordinary differential equations

The DQM is a numerical solution technique for initial and/or boundary value problems [35]. It was first developed by Richard Bellman and his associates in the early 1970's [36]. The DQM is originated from the idea of conventional integral quadrature and approximates the derivative of a function, with respect to a apace variable at a given discrete point, by a weighted linear sum of the function values at all of the discrete points in the domain of that variable [37]. Let $f(y)$ be a solution of a differential equation and $y_1, y_2, ..., y_m$ be a set of sample points in the *y*-direction. According to the DQM, the second- and fourth-order derivatives of the function $f(y)$ at any sample point can be expressed by the following formulations [35-37]

$$f_{,yy}(y_i) = \sum_{j=1}^{m} E^{(2)}_{ij} f(y_j),\quad f_{,yyyy}(y_i) = \sum_{j=1}^{m} E^{(4)}_{ij} f(y_j) \tag{20}$$

where $f(y_j)$ represents the function value at the discrete point y_j, $f_{,yy}(y_i)$ and $f_{,yyyy}(y_i)$ indicate the second- and fourth-order derivatives of $f(y,t)$ at the discrete point y_i, and $E^{(r)}_{ij}$ (r = 2, 4) are the weighting coefficients of the *r*th-order derivative.

The DQ rules for the second- and fourth-order derivatives of the vector $\{W(y)\}$ can be expressed as [30-33, 38-43]

$$\{W_{,yy}(y_i)\} = \sum_{j=1}^{m} E_{ij}^{(2)}\{W(y_j)\}, \quad \{W_{,yyyy}(y_i)\} = \sum_{j=1}^{m} E_{ij}^{(4)}\{W(y_j)\} \tag{21}$$

Satisfying Eq. (19) at any sample point y_i, one has

$$D_{11}[A]\{W(y_i)\} + 2\lambda^2[C]\{W_{,yy}(y_i)\} + \lambda^4 D_{22}[B]\{W_{,yyyy}(y_i)\} + \Omega^2[B]\{W(y_i)\} + 2v\Omega[D]\{W(y_i)\} + v^2[C]\{W(y_i)\} = N_x(y_i)[C]\{W(y_i)\}, \quad i = 1,2,...,m \tag{22}$$

Let the size of matrices appeared in Eq. (22) be $q \times q$. Substituting the quadrature rules, given in Eq. (21), into Eq. (22) yields

$$D_{11}[A]\{W(y_i)\} + 2\lambda^2[C]\sum_{j=1}^{m} E_{ij}^{(2)}\{W(y_i)\} + \lambda^4 D_{22}[B]\sum_{j=1}^{m} E_{ij}^{(4)}\{W(y_i)\} + \Omega^2[B]\{W(y_i)\} + 2v\Omega[D]\{W(y_i)\} + v^2[C]\{W(y_i)\} = N_x(y_i)[C]\{W(y_i)\}, \quad i = 1,2,...,m \tag{23}$$

Eq. (23) may be written in compact form as

$$\left([\tilde{K}] + \Omega[\tilde{C}] + \Omega^2[\tilde{M}]\right)\{\tilde{W}\} = \{\tilde{0}\} \tag{24}$$

where the $q \times q$ sub-matrices $[\tilde{M}_{ij}]$, $[\tilde{K}_{ij}]$, and $[\tilde{C}_{ij}]$, also the $q \times 1$ sub-vector $\{\tilde{W}_i\}$ are given by

$$[\tilde{M}_{ij}] = I_{ij}[B], \quad i, j = 1,2,...,m \tag{25}$$

$$[\tilde{K}_{ij}] = D_{11}I_{ij}[A] + 2\lambda^2 E_{ij}^{(2)}[C] + \lambda^4 D_{22}E_{ij}^{(4)}[B] + v^2 I_{ij}[C] - N_x(y_i)I_{ij}[C] \tag{26}$$

$$[\tilde{C}_{ij}] = 2vI_{ij}[D] \tag{27}$$

$$\{\tilde{W}_i\} = \{W(y_i)\} \tag{28}$$

wherein I_{ij} are the elements of the $m \times m$ identity matrix. After applying the boundary conditions to Eq. (24), one can solve the resulting generalized eigenvalue problem for the eigenvalues Ω. It is noted that the implementation of boundary conditions is similar to that of one-dimensional beam governing discretized equations (see Refs. [35, 37] and Appendix A for detail).

The vibration and stability characteristics of axially moving orthotropic plates can be investigated from the eigenvalues Ω of the generalized eigenvalue problem (24). The eigenvalues Ω of the matrix equations (24) are complex in general, and can be expressed in the form

$$\Omega = \mathrm{Re}(\Omega) \pm \mathrm{Im}(\Omega) \tag{29}$$

The types of instabilities of a moving plate can then be determined from the eigenvalues Ω, as follows [1-19]:

$$\begin{aligned}&\text{Stable if } \mathrm{Re}(\Omega) \le 0\\ &\text{Divergence instability if } \mathrm{Re}(\Omega) > 0 \text{ and } \mathrm{Im}(\Omega) = 0\\ &\text{Flutter instability if } \mathrm{Re}(\Omega) > 0 \text{ and } \mathrm{Im}(\Omega) \ne 0\end{aligned} \tag{30}$$

4. Numerical results and discussion

To demonstrate the stability, rate of convergence and accuracy of the proposed formulation, two numerical examples are first presented. The numerical examples are of the vibration and buckling problems of isotropic and orthotropic rectangular plates for which accurate analytical or numerical solutions are available in the literature. Therefore, these two examples serve well to assess the numerical accuracy of the proposed method. In order to simplify the notations, the boundary conditions for plates are denoted by a four-letter symbol. For convenience, S, C and F in a four-letter symbol are denoted as a simply supported, a clamped and a free edge supports, respectively. For instance, the symbol CFCF denotes that the plate is clamped at $x = 0$ and $x = a$, and free at $y = 0$ and $y = b$.

In the third and fourth examples, the dynamic behavior of axially moving single-span and multi-span orthotropic plates subjected to linearly varying inplane stresses is investigated and the effects of following factors having something to do with the title problem are studied: the moving speed, variation of inplane stresses, and material properties of the orthotropic plate.

In solving the test problems, the problem domain along x-direction is divided into n number of equal length finite elements with pth order interpolation functions, and m number of DQM sampling points are considered in the y-direction. Moreover, the DQM sampling points are taken non-uniformly spaced and are given by the following equations [35]

$$\begin{aligned}&y_1 = 0,\ y_2 = \delta \times b,\\ &y_i = b/2\left[1 - \cos\left(\frac{(i-2)\pi}{m-3}\right)\right], \quad i = 3,4,\ldots,m-2\\ &y_{m-1} = (1-\delta)\times b,\ y_m = b\end{aligned} \tag{31}$$

where y_2 and y_{m-1} are discrete points very close to the boundary points (adjacent δ-points), and b is the plate dimension in the y direction. This type of sampling points was firstly introduced by Bert and Malik [35]. In solving the free vibration and buckling problems of orthotropic rectangular plates, the present authors showed that the DQ solutions with this type of sample points produce better accuracy than the commonly used uniform and non-uniform sample points [30]. In this work, the DQ results are obtained using $\delta = 10^{-3}$.

4.1. Example 1: Free vibration and buckling of an isotropic rectangular plate

The first six frequency parameters for an isotropic square clamped plate are calculated using different values of n (number of finite elements), p (order of interpolation functions), and m (number of DQM sampling points). Table 1 demonstrates the converging trend of solutions with increasing p and m. Only *one finite element* is considered in the x-direction. The results of mixed Ritz-DQM [32], Ritz method [44], discrete singular convolution (DSC) method [45], and differential quadrature method [45] are also shown for comparison. It can be seen that the present results converge very quickly and agree very well with existing literature data. It can also be seen that a reasonable accurate results is obtained by the present method when $m \geq 15$. Table 2 presents the convergence behavior of solutions with respect to p and n. It can be seen that the convergence rate of the present method is not very satisfactory when Hermite interpolation functions are used in the algorithm (i.e., when $p = 3$). Therefore, to accelerate the convergence rate of the method, one should use at least $p = 5$ in the algorithm. It has also to be pointed out that no numerical difficulties are encountered in the present formulation even when a large number of finite elements with high-order interpolating functions are considered. This is very advantageous compared to the conventional DQ-Ritz methodology (see Refs. [31-33]) wherein simple polynomial functions with large arguments (directly proportional to p) result in a very ill-posed problem. In Table 3, the results of the proposed formulation are compared with the Ritz-DQM solutions [32], and the Ritz solutions of Leissa [44] for different boundary conditions of the plate. It can be seen that the natural frequencies are in close agreement with those of Leissa [44], however slightly smaller, which should be so as the Ritz method essentially represents an upper bound limits. Moreover, the present results for CCSF and CFSF plates are smaller than the corresponding ones by the mixed Ritz-DQM which means the present method is more accurate than the mixed Ritz-DQM. On the other hand, the rate of convergence of the present method for plates with free edges is not as high as that for plates without free edges, as to be expected.

To demonstrate the capability of the proposed mixed methodology in prediction of high-order eigenmodes of rectangular plates, the first 100 eigenfrequencies of a SSSS square plate are calculated by the present method. The application is made only to SSSS square plates since the explicit exact solution exists only for this case. The numerical results for the 10th, 20th, 30th, 40th, 50th, 60th, 70th, 80th, 90th and 100th eigenfrequencies are tabulated in Tables 4 and 5. The corresponding analytical values of eigenfrequencies are also shown for comparison. It can be observed from Tables 4 and 5 that the present results agree well with analytical solutions for all modes. Besides, a larger values of n, m and p are required to be used to accurately compute the higher order eigenmodes.

To validate the present formulation for buckling analysis of plates subjected to non-uniform distributed in-plane loadings, application is made to a numerical example given by Civalek et al. [46]. The plate is isotropic and subjected to a distributed load in the form

$$N_x = N_0 f(y) = N_0 \left(1 - \alpha \frac{y}{b}\right) \tag{32}$$

Tables 6 and 7 shows the converging trend of the normalized critical compressive loads with increasing n, p and m for SSSS and SCSC square plates, respectively. The results are compared with the Ritz-DQM solutions of Jafari and

Eftekhari [30] and the DSC results of Civalek et al. [46]. The results have a close agreement with those of existing literature. Besides, by increasing the order of interpolation functions, a smaller number of finite elements are required to obtain solutions with identical accuracies. Again, one sees that the rate of convergence of the present method is not very satisfactory when Hermite interpolation functions are used in the algorithm.

In Table 8, the results are given for different aspect ratios (a/b). As it is evident from this table, the results obtained by the present methodology have closer agreements with the Ritz-DQM solutions of Jafari and Eftekhari [30] than those of Civalek et al. [46]. In Table 9, the present results are compared with the DSC results of Civalek et al. [46], the DQM solution results of Wang et al. [47], and the analytical solutions of Leissa and Kang [48]. Excellent agreement is achieved between the present algorithm solutions and those of existing literature.

4.2. Example 2: Free vibration of an orthotropic rectangular plate

In Table 10, the convergence and accuracy of the fundamental frequency of a clamped orthotropic rectangular plate are verified. Only *one finite element* is used to obtain the results in present analysis. The material properties of the plate are assumed to be: $D_{33} = D_{22} = 1.5D_{11}$. In this Table, the results of two superposition methods are also shown for comparisons [49, 50]. It is seen that the frequency parameters generated from this study agree well with the Levy-type solution results from Refs. [49, 50].

Table 11 presents the validation of proposed method for free vibration analysis of an orthotropic CCCC plate with initial stresses. The material properties of the orthotropic plate are: $D_{11} = D_{22} = 2D_{33}$. Good agreement is observed between the results of the method presented here and those from Refs. [50, 51].

4.3. Example 3: Free vibration of an axially moving single-span orthotropic rectangular plate subjected to linearly varying inplane stresses

To investigate the effects of dimensionless moving speed, material properties of the plate, variation of inplane stresses, and the aspect ratio on the stability property of the moving plate, we consider a single-span rectangular plate with all edges simply supported (SSSS). The real and imaginary parts of the first three dimensionless complex frequencies are obtained for different dimensionless axially moving speeds. Only *one finite element* with 13th order interpolation functions is considered in the *x*-direction, and 17 DQM sampling points are adopted in the *y*-direction. In Fig. 3, the variations of the first three complex natural frequencies of the SSSS isotropic plate with axially moving speed are shown. It can be observed that, when axially moving speed is zero, the real parts of all natural frequencies are zero. By increasing the moving speed, the imaginary parts decrease, while their real parts remain zero. Note that for the moving speed lower than v = 6.29 all eigenvalues are pure imaginary and therefore the moving plate is stable. At v = 6.29, which is called critical or divergence velocity, the imaginary part of Ω_1 becomes zero while the real part starts to take positive and negative values. After that, some values of the real part of Ω_1 may exceed the zero magnitude and therefore the moving plate will experience the divergent instability. In this case, a bubble is formed with bifurcation and reverse bifurcation in

the plot. If the moving speed falls within the bubble, the moving plate will be unstable as the plate vibration amplitude would grow significantly with time. From Fig. 3, it can also be seen that there exists a second stable region where all eigenvalues become pure imaginary. At v = 8.23, which is called flutter velocity, the real parts of Ω_1 and Ω_2 start to take positive and negative values while their imaginary parts are non-zero. If the moving speed is further increased, a larger bubble is formed with bifurcation in the plot. In this case, the real and imaginary parts of Ω_1 couples with those of Ω_2 which means the plate will experience coupled-mode flutter and loses stability for the second time.

Figs. 4 and 5 show the variation of the first three dimensionless complex frequencies of the orthotropic plate versus moving speed for various values of plate flexural rigidities. From Fig. 4 it is seen that the divergence velocity and flutter velocity both increases by increasing the D_{11}-value. It can also be seen that the size of the first bubble increases considerably as the D_{11}-value increases. This means while an increase in D_{11}-value will improve the dynamic behavior of axially moving orthotropic plates, it increases the instability limit of the first unstable region. However, the instability limit of the first coupled-mode flutter decreases as the D_{11}-value increases (note that Ω_1 does not couple with Ω_2 when $D_{11} = 4D_{33}$).

From Fig. 5, it can be seen that an increase in D_{22}-value can also improve the dynamical behavior of axially moving orthotropic plates (i.e., the divergence and flutter velocities increase as the D_{22}-value increases). It can also be seen that as D_{22}-value increases, the size of the first bubble decreases. Note that the first bubble is vanished when $D_{22} = 4D_{33}$. In summary, from the results shown in Figs. 4 and 5, one may conclude that the vibrational behavior of axially moving orthotropic plates can be easily controlled by choosing the proper values of the flexural rigidities.

Fig. 6 shows the variation of the first three dimensionless complex frequencies of the orthotropic plate with moving speed for different aspect ratios. It can be observed that the divergence and flutter velocities increase as the aspect ratio increases. Moreover, the size of the first bubble decreases significantly as the aspect ratio increases.

Figs. 7 and 8 demonstrate the effects of inplane stresses and their variation on stability of the axially moving orthotropic plate. It can be seen that the divergence and flutter velocities increase as N_0 increases or α decreases. But, the size of first bubble (say first unstable region) does not change as the magnitude of N_0 or α changes. Moreover, the shape of curves does not change by any variation in magnitudes of N_0 and α. In other words, the curves are only shifted to the right direction as N_0 increases or α decreases. Fig. 9 shows the variation of critical velocity with α for different values of N_0. It can be seen that the critical velocity first decreases by increasing α and takes its minimum value. After that, the critical velocity increases rapidly with increasing α.

4.4. Example 4: Free vibration of an axially moving multi-span orthotropic rectangular plate subjected to linearly varying inplane stresses

Consider an axially moving multi-span SFSF rectangular orthotropic plate with equal length spans subjected to linearly varying inplane stresses. Fig. 10 shows the variation of the first three dimensionless complex frequencies of the orthotropic plates of one, two, and three equal spans versus moving speed. The aspect ratio and material properties of the

orthotropic plate are, respectively, $\lambda = 3$ and $D_{11} = D_{22} = 2D_{33}$. It can be seen that the divergence speeds of the orthotropic plate increase considerably as the number of spans increases. Moreover, for the range of moving speeds shown in this figure, one sees that the single span orthotropic plate is the only one that may experience coupled mode flutter. In conclusion, the dynamic behavior of axially moving plates can be easily improved by increasing the number of spans.

5. Conclusions

A high order accurate mixed FE-DQM is proposed to study the dynamic behavior of axially moving orthotropic rectangular plates loaded by linearly varying inplane stresses. The mixed method reduces the original plate problem to two simple beam problems whose assembly of equations and implementation of boundary conditions are easier than the case where each component method is fully applied to the problem. The numerical examples prove the accuracy, convergence, and stability of the proposed method for the dynamic analysis of axially moving orthotropic rectangular plates.

The effects of material properties of the orthotropic plate, axial moving speed, magnitude and variation of inplane stresses on the dynamics of the moving plate are also investigated. It is found that all the above-mentioned parameters have significant effects on the dynamic behavior of moving orthotropic plates. Results indicate that the critical velocity of the orthotropic plates can be easily controlled by choosing the proper values of flexural rigidities of the plate, inplane stresses and their variation along plate boundaries.

References

[1] Wickert, J. and Mote Jr, C.D. "Classical vibration analysis of axially moving continua", *ASME J. Appl. Mech*., **57**, pp. 738-744 (1990).

[2] Tan, C.A. and Ying, S. "Dynamic analysis of the axially moving string based on wave propagation", *ASME J. Appl. Mech*., **64**, pp. 394-400 (1997).

[3] Zhu, W.D. and Guo, B.Z. "Free and forced vibration of an axially moving string with an arbitrary velocity profile", *ASME J. Appl. Mech*., **65**, pp. 901-907 (1998).

[4] Pellicano, F. and Vestroni, F. "Nonlinear dynamics and bifurcations of an axially moving beam", *ASME J. Vib. Acoust*., **122**, pp. 21-30 (2000).

[5] Lee, U., Kim, J. and Oh, H. "Spectral analysis for the transverse vibration of an axially moving Timoshenko beam", *J. Sound Vib.*, **271**, pp. 685-703 (2004).

[6] Chen, L.Q. "Analysis and control of transverse vibrations of axially moving strings", *ASME Appl. Mech. Rev*., **58**, pp. 91-116 (2005).

[7] Ghayesh, M.H. and Khadem, S.E. "Rotary inertia and temperature effects on non-linear vibration, steady-state response and stability of an axially moving beam with time-dependent velocity", *Int. J. Mech. Sci*., **50**, pp. 389-404 (2008).

[8] Guo, X-X., Wang, Z-M., Wang, Y. and Zhou, Y-F. "Analysis of the coupled thermoelastic vibration for axially moving beam", *J. Sound Vib*., **325**, pp. 597-608 (2009).

[9] Guo, X-X. and Wang, Z-M. "Thermoelastic coupling vibration characteristics of the axially moving beam with frictional contact", *ASME J. Vib. Acoust*., **132**, 051010 (2010).

[10] Lin, C.C. "Stability and vibration characteristics of axially moving plates", *Int. J. Solids Struct*., **34**, 3179-90 (1997).

[11] Lou, Z. and Hutton, S.G. "Formulation of a three-node traveling triangular plate element subjected to gyroscopic and in-plane forces", *Comput. Struct*., **80**, pp. 1935-1944 (2002).

[12] Kim, J., Cho, J., Lee, U. and Park, S. "Modal spectral element formulation for axially moving plates subjected to in-plane axial tension", *Comput. Struct*., **81**, pp. 2011-2020 (2003).

[13] Zhou, Y-F. and Wang, Z-M. "Transverse vibration characteristics of axially moving viscoelastic plate", *Appl. Math. Mech. Engl. Ed*., **28**(2), pp. 209-218 (2007).

[14] Hatami, S., Azhari, M. and Saadatpour, M.M. "Free vibration of moving laminated composite plates", *Compos. Struct*., **80**, pp. 609-620 (2007).

[15] Hatami, S., Ronagh, H.R. and Azhari, M. "Exact free vibration analysis of axially moving viscoelastic plates", *Comput. Struct*., **86**, 1738-1746 (2008).

[16] Banichuk, N., Jeronen, J., Neittaanmäki, P. and Tuovinen, T. "On the instability of an axially moving elastic plate", *Int. J. Solids Struct*., **47**, pp. 91-99 (2010).

[17] Wang, L., Hu, Z. and Zhong, Z. "Dynamic analysis of an axially translating plate with time-variant length", *Acta Mech*., **215**, pp. 9-23 (2010).

[18] Marynowsky, K. "Free vibration analysis of the axially moving Levy-type viscoelastic plate", *Eur. J. Mech. A-Solids*, **29**, pp. 879-886 (2010).

[19] Yang, X-D., Chen, L-Q. and Zu, J.W. "Vibrations and stability of an axially moving rectangular composite plate", ASME J. Appl. Mech., 78, 011018 (2011).

[20] Bert, C.W., Kang, S.K. and Striz, A. G. "Two new approximate methods for analyzing free vibration of structural components", *AIAA J.*, **26**, pp. 612–618 (1988).

[21] Bert, C.W., Wang, X. and Striz, A.G. "Differential quadrature analysis of deflection, buckling, and free vibration of beams and rectangular plates", *Comput. Struct*., **48**(3), pp. 473–479 (1993).

[22] Du, H., Liew, K.M. and Lim, M.K. "Generalized differential quadrature method for buckling analysis", *J. Engrg. Mech*., **122**, pp. 95–100 (1996).

[23] Civalek, Ö. "Application of differential quadrature (DQ) and harmonic differential quadrature (HDQ) for buckling analysis of thin isotropic plates and elastic columns", *Engrg. Struct*., **26**(2), pp. 171-186 (2004).

[24] Sakata T., Takahashi, K. and Bhat, R.B. "Natural frequencies of orthotropic rectangular plates obtained by iterative reduction of the partial differential equation", *J. Sound Vib*., **189**(1), pp. 89–101 (1996).

[25] Wei, G. W. "Vibration analysis by discrete singular convolution", *J. Sound Vib*., **244**(3), pp. 535-553 (2001).

[26] Civalek, Ö, "A four-node discrete singular convolution for geometric transformation and its application to numerical solution of vibration problem of arbitrary straight-sided quadrilateral plates", *Appl. Math. Model*., **33**(1), pp. 300-314 (2009).

[27] Alipour, M.M., Shariyat, M. and Shaban, M. "A semi-analytical solution for free vibration and modal stress analyses of circular plates resting on two-parameter elastic foundations", *J. Solid Mech*., **2**(1), pp. 63-78 (2010).

[28] Xing, Y. and Liu, B. "High-accuracy differential quadrature finite element method and its application to free vibrations of thin plate with curvilinear domain", *Int. J. Numer. Methods Engrg*., **80**, pp. 1718–1742 (2009).

[29] Xing, Y., Liu, B. and Liu, G. "A differential quadrature finite element method", *Int. J. Appl. Mech*., 2(1), pp. 1-20 (2010).

[30] Jafari, A.A. and Eftekhari, S.A. "An efficient mixed methodology for free vibration and buckling analysis of orthotropic rectangular plates", *Appl. Math. Comput*., **218**, pp. 2670-2692 (2011).

[31]] Eftekhari, S.A. and Jafari, A.A. "Vibration of an initially stressed rectangular plate due to an accelerated traveling mass", *Sci. Iran. A*, **19**(5), pp. 1195–1213 (2012).

[32] Eftekhari, S.A. and Jafari, A.A. "A mixed method for free and forced vibration of rectangular plates", *Appl. Math. Model*., **36**, pp. 2814–2831 (2012).

[33] Eftekhari, S.A. and Jafari, A.A. "Mixed finite element and differential quadrature method for free and forced vibration and buckling analysis of rectangular plates", *Appl. Math. Mech. Engl. Ed*., **33**(1), pp. 81–98 (2012).

[34] Reddy, J.N. *An Introduction to the Finite Element Method*, McGraw-Hill Inc., NY (1993).

[35] Bert, C.W. and Malik, M. "Differential quadrature method in computational mechanics: A review", *ASME Appl. Mech. Rev*., **49**, pp. 1–28 (1996).

[36] Bellman, R.E. and Casti, J. "Differential quadrature and long term integrations", *J. Math. Anal. Appl*., **34**, pp. 235–238 (1971).

[37] Shu, C. *Differential Quadrature and Its Application in Engineering*, Springer, NY (2000).

[38] Eftekhari, S.A., Farid, M. and Khani, M. "Dynamic analysis of laminated composite coated beams carrying multiple accelerating oscillators using a coupled finite element-differential quadrature method", *ASME J. Appl. Mech*., **76**, 061001 (2009).

[39] Eftekhari, S.A. and Khani, M. "A coupled finite element-differential quadrature element method and its accuracy for moving load problem", *Appl. Math. Model*., **34**, pp. 228–237 (2010).

[40] Khalili, S.M.R., Jafari, A.A. and Eftekhari, S.A. "A mixed Ritz-DQ method for forced vibration of functionally graded beams carrying moving loads", *Compos. Struct*., **92**(10), pp. 2497-2511 (2010).

[41] Jafari, A.A. and Eftekhari, S.A. "A new mixed finite element-differential quadrature formulation for forced vibration of beams carrying moving loads", *ASME J. Appl. Mech*., **78**(1), 011020 (2011).

[42] Eftekhari, S.A. and Jafari, A.A. "Coupling Ritz method and triangular quadrature rule for moving mass problem", *ASME J. Appl. Mech*., **79**(2), 021018 (2012).

[43] Eftekhari, S.A. and Jafari, A.A. "Modified mixed Ritz-DQ formulation for free vibration of thick rectangular and skew plates with general boundary conditions", *Appl. Math. Model*., **37**, pp. 7398–7426 (2013).
[44] Leissa, A.W. "The free vibration of rectangular plates", *J. Sound Vib*., **31**(3), pp. 257-293 (1973).
[45] Ng, C.H.W., Zhao Y.B., and Wei G.W. "Comparison of discrete singular convolution and generalized differential quadrature for the vibration analysis of rectangular plates", *Comput. Methods Appl. Mech. Engrg*., **193**, pp. 2483–2506 (2004).
[46] Civalek, Ö., Korkmaz, A. and Demir, C. "Discrete singular convolution approach for buckling analysis of rectangular Kirchhoff plates subjected to compressive loads on two-opposite edges", *Adv. Eng. Soft*., **41**, pp. 557–560 (2010).
[47] Wang, X., Gan, L. and Wang, Y. "A differential quadrature analysis of vibration and buckling of an SS-C-SS-C rectangular plate loaded by linearly varying in−plane stresses", *J. Sound Vib*., **298**(1–2), pp. 420–431 (2006).
[48] Leissa, A.W. and Kang, J.H. "Exact solutions for vibration and buckling of an SS-C-SS-C rectangular plate loaded by linearly varying in-plane stresses", *Int. J. Mech. Sci*., **44**, 1925–1945 (2002).
[49] Gorman, D.J. "Accurate free vibration analysis of clamped orthotropic plates by the method of superposition", *J. Sound Vib*., **140**, pp. 391-411 (1990).
[50] Kshirsagar, S. and Bhaskar, K. "Accurate and elegant free vibration and buckling studies of orthotropic rectangular plates using untruncated infinite series", *J. Sound Vib*., **314**, pp. 837–850 (2008).
[51] Dickinson, S.M. "The flexural vibration of rectangular orthotropic plates subjected to in-plane forces", *ASME J. Appl. Mech*., **38**, pp. 699–700 (1971).

Seyyed Aboozar Eftekhari was born in Karaj, Iran, in 1980. He received a BS degree in Mechanical Engineering from Sharif University of Technology, Tehran, Iran, in 2003, an MS degree in Mechanical Engineering from Shiraz University, Shiraz, Iran, in 2006, and a PhD degree in Mechanical Engineering from K. N. Toosi University of Technology, Tehran, Iran, in 2013.

He is currently a member of Young Researchers and Elite Club, Karaj Branch, Islamic Azad University, Karaj, Iran. His research interests include applied mathematics, time integration schemes, vibration of continuous systems, and fluid-structure interaction. He has published over 20 research papers on related subjects, including the study of the behavior of beams and plates under moving loads, mathematical modeling of vibration problem of beams and plates, and numerical solution of nonlinear differential equations in engineering and applied sciences.

Ali Asghar Jafari received his Ph. D. degree in Mechanical Engineering from University of Wollongong, Australia, in 1994. Dr. Jafari is currently a full professor in the Department of Mechanical Engineering at K.N. Toosi University of Technology, Iran. His research fields are dynamics and vibrations of beams, plates and shells, composite structures and automotive engineering.

Appendix A

In this study, the technique of direct Substitution of Boundary Conditions into discrete Governing Equations (SBCGE) [37] is used to implement the boundary conditions of the plate problem in y direction. In this technique, the plate boundary conditions are first discretized using the DQ approach. The resulting analog equations are then substituted into discrete governing equations (24) (for more details, see Refs. [35, 37]).

The boundary conditions of the orthotropic plate are given in Eqs. (3)-(8). Using the differential quadrature rules (21), the corresponding quadrature analogs are obtained as:

(I) Simply supported end condition at $y = y_r$ (r =1 or m)

$$\{W(y_r)\} = \begin{Bmatrix} W_1(y_r) \\ W_2(y_r) \\ \cdot \\ \cdot \\ \cdot \\ W_q(y_r) \end{Bmatrix} = \begin{Bmatrix} 0 \\ 0 \\ \cdot \\ \cdot \\ \cdot \\ 0 \end{Bmatrix} = \{0\} \tag{A.1}$$

$$\{W_{,yy}(y_r)\} = \sum_{j=1}^{m} E_{rj}^{(2)} \{W(y_j)\} = \{0\} \tag{A.2}$$

(II) Clamped or fixed end condition at $y = y_r$ (r =1 or m)

$$\{W(y_r)\} = \{0\} \tag{A.3}$$

$$\{W_{,y}(y_r)\} = \sum_{j=1}^{m} E_{rj}^{(1)} \{W(y_j)\} = \{0\} \tag{A.4}$$

(III) Free end condition at $y = y_r$ (r =1 or m)

$$D_{22}[B] \sum_{j=1}^{m} E_{rj}^{(2)} \{W(y_j)\} + D_{12}[C]\{W(y_r)\} = \{0\} \tag{A.5}$$

$$D_{22}[B] \sum_{j=1}^{m} E_{rj}^{(3)} \{W(y_j)\} + (2D_{33} - D_{12})[C] \sum_{j=1}^{m} E_{rj}^{(1)} \{W(y_j)\} = \{0\} \tag{A.6}$$

where the matrices $[B]$ and $[C]$ are defined in Eqs. (18) and (19).

Table captions

Table 1 Convergence of natural frequencies ($\Omega_i = \omega_i a^2\sqrt{\rho h/D}$) of an isotropic CCCC square plate (n = 1)

Table 2 Convergence of natural frequencies ($\Omega_i = \omega_i a^2\sqrt{\rho h/D}$) of an isotropic CCCC square plate (m = 17)

Table 3 Convergence of natural frequencies ($\Omega_i = \omega_i a^2\sqrt{\rho h/D}$) of square isotropic plates with different boundary conditions (n = 1, m=19)

Table 4 Convergence of natural frequencies ($\Omega_i = \omega_i a^2\sqrt{\rho h/D}$) of an isotropic SSSS square plate (n = 5)

Table 5 Convergence of natural frequencies ($\Omega_i = \omega_i a^2\sqrt{\rho h/D}$) of an isotropic SSSS square plate (m = 35)

Table 6 Convergence of buckling load (Na^2/D) of an isotropic SSSS square plate under uniaxial linearly varying compressive load (α = 1)

Table 7 Convergence of buckling load (Na^2/D) of an isotropic SCSC square plate under uniaxial linearly varying compressive load (α = 0.25)

Table 8 Convergence of buckling load (Na^2/D) of isotropic SSSS square plates under uniaxial linearly varying compressive load (n = 1, p = 9, m = 16)

Table 9 Non-dimensional critical buckling loads (Na^2/D) for SCSC isotropic rectangular plate under different linearly varying compressive loads (n = 1, p = 9, m = 16, a/b = 0.7)

Table 10 Convergence of fundamental frequency ($\Omega_1 = \omega_1 a^2\sqrt{\rho h/D_{11}}$) of an orthotropic CCCC plate ($D_{33} = D_{22} = 1.5D_{11}$, n = 1)

Table 11 Convergence of fundamental frequency ($\Omega_1 = \omega_1 a^2\sqrt{\rho h/D_{33}}$) of an square orthotropic CCCC plate with initial stresses ($D_{11} = D_{22} = 2D_{33}$, $N_x = N_y = N$, n = 1)

Figure captions

Fig. 1 Geometry and co-ordinate system for an axially moving orthotropic plate with (N – 1) internal line supports subjected to a non-uniform inplane axial force (tension)

Fig. 2 A single span rectangular plate under different types of edge loading: (a) α = 0; (b) α = 1; (c) α = 2.

Fig. 3 Dimensionless complex frequencies of axially moving single-span isotropic SSSS square plates versus axially moving speed.

Fig. 4 Dimensionless complex frequencies of axially moving single-span orthotropic SSSS square plates versus axially moving speed for different values of D_{11}.

Fig. 5 Dimensionless complex frequencies of axially moving single-span orthotropic SSSS square plates versus axially moving speed for different values of D_{22}.

Fig. 6 Dimensionless complex frequencies of axially moving single-span orthotropic SSSS rectangular plates versus axially moving speed for different values $\lambda = a/b$.

Fig.7 Dimensionless complex frequencies of axially moving single-span orthotropic SSSS rectangular plates versus axially moving speed for different values of inplane forces ($D_{11} = D_{22} = 2D_{33}$, $\lambda = 3/2$, $\alpha = 0$)

Fig.8 Dimensionless complex frequencies of axially moving single-span orthotropic SSSS rectangular plates versus axially moving speed for different values of α ($D_{11} = D_{22} = 2D_{33}$, $\lambda = 3/2$, $N_0a^2/D_{33} = 100$)

Fig.9 Variation of critical velocity of an axially moving single-span orthotropic SSSS rectangular plates versus α-value for different values of N_0 ($D_{11} = D_{22} = 2D_{33}$, $\lambda = 3/2$).

Fig.10 Dimensionless complex frequencies of axially moving multi-span orthotropic SFSF rectangular plates versus axially moving speed ($D_{11} = D_{22} = 2D_{33}$, $\lambda = 3$, $N_0a^2/D_{33} = 100$, $\alpha = 1$)

Table 1

Convergence of natural frequencies ($\Omega_i = \omega_i a^2\sqrt{\rho h/D}$) of an isotropic CCCC square plate (n = 1)

p	Ω	m=11	m=13	m=15	m=17	m=19	m=21	Ritz-DQ [32]	Ritz [44]	DSC-LK [45]	GDQ [45]
5	1	35.9995	35.9995	35.9995	35.9995	35.9995	35.9995				
	2	73.5388	73.5346	73.5345	73.5345	73.5345	73.5345				
	3	74.1799	74.1797	74.1797	74.1797	74.1797	74.1797				
	4	108.4156	108.4112	108.4111	108.4111	108.4111	108.4111				
	5	131.6220	132.2532	132.2604	132.2604	132.2604	132.2604				
7	1	35.9882	35.9881	35.9881	35.9881	35.9881	35.9881				
	2	73.4082	73.4037	73.4037	73.4037	73.4037	73.4037				
	3	73.4122	73.4118	73.4118	73.4118	73.4118	73.4118				
	4	108.2436	108.2388	108.2386	108.2386	108.2386	108.2386				
	5	131.2626	131.8946	131.9018	131.9019	131.9019	131.9019				
9	1	35.9855	35.9854	35.9854	35.9854	35.9854	35.9854				
	2	73.3946	73.3941	73.3941	73.3941	73.3941	73.3941				
	3	73.3992	73.3947	73.3946	73.3946	73.3946	73.3946				
	4	108.2222	108.2177	108.2175	108.2174	108.2174	108.2174				
	5	131.1522	131.6599	131.6645	131.6646	131.6646	131.6646				
	6	132.1960	132.3207	132.3232	132.3232	132.3232	132.3232				
11	1	35.9853	35.9852	35.9852	35.9852	35.9852	35.9852				
	2	73.3943	73.3939	73.3939	73.3939	73.3939	73.3939				
	3	73.3984	73.3940	73.3939	73.3939	73.3939	73.3939				
	4	108.2209	108.2170	108.2167	108.2166	108.2166	108.2166				
	5	131.1293	131.5780	131.5815	131.5816	131.5816	131.5816				
	6	132.0197	132.2024	132.2060	132.2060	132.2060	132.2060				
13	1	35.9853	35.9852	35.9852	35.9852	35.9852	35.9852				
	2	73.3943	73.3939	73.3939	73.3938	73.3938	73.3938				
	3	73.3982	73.3940	73.3939	73.3939	73.3939	73.3939				
	4	108.2207	108.2168	108.2166	108.2165	108.2165	108.2165				
	5	131.1293	131.5772	131.5807	131.5808	131.5808	131.5808				
	6	132.0182	132.2012	132.2049	132.2049	132.2049	132.2049				
15	1	35.9853	35.9852	35.9852	35.9852	35.9852	35.9852	35.9852	35.992	35.989	35.985
	2	73.3943	73.3939	73.3939	73.3938	73.3938	73.3938	73.3939	73.413	73.407	73.394
	3	73.3982	73.3939	73.3939	73.3939	73.3939	73.3939	73.3939	73.413	73.407	73.394

	4	108.2207	108.2168	108.2165	108.2165	108.2165	108.2165	108.216	108.27	108.249	108.210
	5	131.1293	131.5772	131.5807	131.5808	131.5808	131.5808	131.581	131.64	131.622	131.580
	6	132.0181	132.2011	132.2048	132.2048	132.2048	132.2048	132.205	132.24	132.244	132.200

Table 2

Convergence of natural frequencies ($\Omega_i = \omega_i a^2\sqrt{\rho h/D}$) of an isotropic CCCC square plate (m = 17)

p	Ω	n=1	n=2	n=3	n=4	n=5	n=10	Ritz-DQ [32]	Ritz [44]	DSC-LK [45]	GDQ [45]
3	1	----------	36.4831	36.0924	36.0219	36.0014	35.9864	35.9852	35.992	35.989	35.985
	2	----------	74.1918	73.6141	73.4826	73.4367	73.3976	73.3939	73.413	73.407	73.394
	3	----------	92.3989	74.7826	73.9463	73.6267	73.4090	73.3939	73.413	73.407	73.394
	4	----------	124.8356	109.9967	108.8522	108.4893	108.2365	108.216	108.27	108.249	108.210
	5	----------	132.9960	132.2569	132.0293	131.9227	131.6376	131.581	131.64	131.622	131.580
	6	----------	179.8715	156.3730	134.6547	133.5760	132.2694	132.205	132.24	132.244	132.200
5	1	35.9995	35.9870	35.9855	35.9853	35.9852	35.9852				
	2	73.5345	73.4019	73.3947	73.3942	73.3940	73.3938				
	3	74.1797	73.4286	73.3952	73.3942	73.3940	73.3938				
	4	108.4111	108.2275	108.2202	108.2177	108.2169	108.2165				
	5	132.2604	131.8262	131.6122	131.5816	131.5812	131.5808				
	6	165.0573	133.0578	132.2411	132.2063	132.2055	132.2048				
7	1	35.9881	35.9852	35.9852	35.9852	35.9852	35.9852				
	2	73.4037	73.3941	73.3939	73.3938	73.3938	73.3938				
	3	73.4118	73.3941	73.3939	73.3938	73.3938	73.3938				
	4	108.2386	108.2175	108.2166	108.2165	108.2165	108.2165				
	5	131.9019	131.5852	131.5808	131.5808	131.5808	131.5808				
	6	137.6816	132.2100	132.2050	132.2048	132.2048	132.2048				
9	1	35.9854	35.9852	35.9852	35.9852	35.9852	35.9852				
	2	73.3941	73.3939	73.3938	73.3938	73.3938	73.3938				
	3	73.3946	73.3939	73.3938	73.3938	73.3938	73.3938				
	4	108.2174	108.2166	108.2165	108.2165	108.2165	108.2165				
	5	131.6646	131.5808	131.5808	131.5808	131.5808	131.5808				
	6	131.3232	132.2049	132.2048	132.2048	132.2048	132.2048				
11	1	35.9852	35.9852	35.9852	35.9852	35.9852	35.9852				
	2	73.3939	73.3938	73.3938	73.3938	73.3938	73.3938				
	3	73.3939	73.3938	73.3938	73.3938	73.3938	73.3938				
	4	108.2166	108.2165	108.2165	108.2165	108.2165	108.2165				
	5	131.5816	131.5808	131.5808	131.5808	131.5808	131.5808				
	6	132.2060	132.2048	132.2048	132.2048	132.2048	132.2048				

Table 3

Convergence of natural frequencies ($\Omega_i = \omega_i a^2\sqrt{\rho h/D}$) of square isotropic plates with different boundary conditions (n=1, m=19)

Plate	Ω	p=5	p=7	p=9	p=11	p=13	p=15	Ritz-DQ [32]	Ritz [44]
CCCS	1	31.834	31.827	31.826	31.826	31.826	31.826	31.826	31.829
	2	63.467	63.338	63.331	63.331	63.331	63.331	63.331	63.347
	3	71.897	71.093	71.076	71.076	71.076	71.076	71.076	71.084
	4	101.010	100.811	100.792	100.792	100.792	100.792	100.793	100.83
	5	116.737	116.385	116.358	116.357	116.357	116.357	116.357	116.40
	6	151.940	136.202	130.553	130.353	130.351	130.351	130.353	130.37
CCSS	1	27.057	27.054	27.054	27.054	27.054	27.054	27.054	27.056
	2	60.656	60.545	60.538	60.538	60.538	60.538	60.538	60.544
	3	61.146	60.793	60.786	60.786	60.786	60.786	60.786	60.791
	4	92.963	92.853	92.836	92.836	92.836	92.836	92.836	92.865
	5	114.725	114.634	114.580	114.556	114.556	114.556	114.556	114.57
	6	146.039	117.241	114.740	114.704	114.704	114.704	114.704	114.72
CCSF	1	17.565	17.545	17.541	17.539	17.538	17.537	17.550	17.615
	2	36.045	36.028	36.025	36.024	36.023	36.023	36.034	36.046
	3	52.538	51.844	51.821	51.816	51.813	51.811	52.238	52.065
	4	71.357	71.101	71.083	71.079	71.077	71.076	71.307	71.194
	5	74.409	74.333	74.327	74.327	74.326	74.326	74.355	74.349
	6	109.477	108.652	105.866	105.794	105.789	105.786	--------	106.28
CFSF	1	15.227	15.199	15.195	15.193	15.192	15.192	15.204	15.285
	2	20.609	20.596	20.590	20.586	20.585	20.584	20.601	20.673
	3	39.780	39.744	39.739	39.737	39.736	39.735	39.755	39.775
	4	50.267	49.480	49.456	49.452	49.449	49.448	49.906	49.730
	5	56.853	56.319	56.293	56.285	56.281	56.278	56.657	56.617
	6	77.456	77.337	77.327	77.325	77.324	77.324	77.369	77.368
CCCF	1	24.028	23.950	23.934	23.926	23.923	23.921	--------	24.020
	2	40.080	40.016	40.006	40.002	39.999	39.998	--------	40.039
	3	64.465	63.279	63.240	63.230	63.224	63.220	--------	63.493
	4	77.042	76.740	76.715	76.712	76.711	76.710	--------	76.761
	5	81.121	80.613	80.585	80.578	80.574	80.571	--------	80.713
	6	116.772	116.700	116.666	116.661	116.657	116.656	--------	116.80
CSCF	1	23.475	23.397	23.382	23.376	23.372	23.371	--------	23.460
	2	35.626	35.588	35.579	35.575	35.573	35.571	--------	35.612

	3	64.124	62.930	62.892	62.883	62.877	62.874	--------	63.126
	4	67.067	66.786	66.767	66.764	66.763	66.762	--------	66.808
	5	77.969	77.414	77.387	77.380	77.376	77.374	--------	77.502
	6	108.988	108.908	108.878	108.873	108.870	108.868	--------	108.99
CFCF	1	22.307	22.193	22.178	22.172	22.169	22.167	--------	22.272
	2	26.484	26.446	26.425	26.415	26.409	26.406	--------	26.529
	3	43.770	43.625	43.608	43.602	43.598	43.595	--------	43.664
	4	62.533	61.230	61.191	61.182	61.177	61.174	--------	61.466
	5	68.219	67.251	67.205	67.189	67.179	67.174	--------	67.549
	6	80.329	79.865	79.825	79.820	79.818	79.816	--------	79.904

Table 4

Convergence of natural frequencies ($\Omega_i = \omega_i a^2\sqrt{\rho h/D}$) of an isotropic SSSS square plate (n = 5)

p	Ω	m=15	m=20	m=25	m=30	m=35	Exact [45]
7	10	167.783275	167.783275	167.783275	167.783275	167.783275	167.783275
	20	315.827693	315.827341	315.827341	315.827341	315.827341	315.827341
	30	446.950054	444.132364	444.132364	444.132364	444.132364	444.132198
	40	601.956821	602.045583	602.045883	602.045883	602.045883	602.045868
	50	785.746316	720.489661	720.489661	720.489661	720.489661	720.481121
	60	882.307481	843.404099	838.959106	838.959106	838.959106	838.916374
	70	1026.45628	986.966798	996.847902	996.830064	996.830044	996.830044
	80	1233.63580	1120.83139	1144.89003	1144.87413	1144.87411	1144.87411
	90	1441.37515	1283.58358	1263.31485	1263.31478	1263.31478	1263.30936
	100	1669.34106	1432.71254	1431.12080	1431.09756	1431.09756	1431.09264
9	10	167.783275	167.783275	167.783275	167.783275	167.783275	
	20	315.827692	315.827341	315.827341	315.827341	315.827341	
	30	446.950054	444.132198	444.132198	444.132198	444.132198	
	40	601.956694	602.045568	602.045868	602.045868	602.045868	
	50	785.746316	720.481128	720.481238	720.481128	720.481128	
	60	882.307481	843.404099	838.916435	838.916435	838.916435	
	70	1026.43888	986.960222	996.830068	996.830064	996.830044	
	80	1233.62084	1120.83139	1144.87413	1144.87412	1144.87411	
	90	1440.88544	1283.06163	1263.30944	1263.30936	1263.30936	
	100	1667.89291	1431.10075	1431.09274	1431.09264	1431.09264	
11	10	167.783275	167.783275	167.783275	167.783275	167.783275	
	20	315.827692	315.827341	315.827341	315.827341	315.827341	
	30	446.950054	444.132198	444.132198	444.132198	444.132198	
	40	601.956694	602.045568	602.045868	602.045868	602.045868	
	50	785.746316	720.481121	720.481238	720.481121	720.481121	
	60	882.307481	843.404099	838.916374	838.916376	838.916374	
	70	1026.43886	986.960216	996.830044	996.830044	996.830044	
	80	1233.62082	1120.83139	1144.87411	1144.87411	1144.87411	
	90	1440.88380	1283.06159	1263.30943	1263.30936	1263.30936	
	100	1667.88575	1431.09265	1431.09265	1431.09264	1431.09264	

Table 5

Convergence of natural frequencies ($\Omega_i = \omega_i a^2\sqrt{\rho h/D}$) of an isotropic SSSS square plate (m = 35)

p	Ω	n=2	n=3	n=4	n=5	n=6	Exact [45]
7	10	167.786014	167.783562	167.783295	167.783275	167.783275	167.783275
	20	315.829004	315.827507	315.827352	315.827341	315.827341	315.827341
	30	449.449016	444.137592	444.134345	444.132364	444.132237	444.132198
	40	602.289841	602.048767	602.045972	602.045883	602.045869	602.045868
	50	730.571272	722.333091	720.491454	720.489661	720.482201	720.481121
	60	888.264520	852.132138	839.375994	838.959106	838.921993	838.916374
	70	1046.36419	996.830044	996.830044	996.830044	996.830044	996.830044
	80	1233.70055	1144.87417	1144.87411	1144.87411	1144.87411	1144.87411
	90	1446.96674	1283.04857	1263.31602	1263.31478	1263.31003	1263.30936
	100	1677.83268	1432.33728	1431.09871	1431.09756	1431.09324	1431.09264
9	10	167.783278	167.783275	167.783275	167.783275	167.783275	
	20	315.827343	315.827341	315.827341	315.827341	315.827341	
	30	444.206377	444.132205	444.132199	444.132198	444.132198	
	40	602.047185	602.045871	602.045868	602.045868	602.045868	
	50	721.260974	720.495892	720.481135	720.481128	720.481122	
	60	852.376378	839.105305	838.918094	838.916435	838.916378	
	70	996.830044	996.830044	996.830044	996.830044	996.830044	
	80	1153.54312	1144.87411	1144.87411	1144.87411	1144.87411	
	90	1294.18941	1263.31922	1263.30937	1263.30936	1263.30936	
	100	1440.96303	1431.10171	1431.09264	1431.09264	1431.09264	
11	10	167.783275	167.783275	167.783275	167.783275	167.783275	
	20	315.827341	315.827341	315.827341	315.827341	315.827341	
	30	444.132552	444.132198	444.132198	444.132198	444.132198	
	40	602.045871	602.045868	602.045868	602.045868	602.045868	
	50	720.490206	720.481162	720.481121	720.481121	720.481121	
	60	839.359817	838.917290	838.916376	838.916374	838.916374	
	70	996.830044	996.830044	996.830044	996.830044	996.830044	
	80	1144.87411	1144.87411	1144.87411	1144.87411	1144.87411	
	90	1263.31560	1263.30939	1263.30936	1263.30936	1263.30936	
	100	1431.09842	1431.09266	1431.09264	1431.09264	1431.09264	

Table 6
Convergence of buckling load (Na^2/D) of a SSSS isotropic square plate under uniaxial linearly varying compressive load ($\alpha = 1$)

n	*p*	*m*=7	*m*=9	*m*=11	*m*=13	*m*=15	Ref. [30]	Ref. [46]
1	3	81.4895	80.8989	80.8987	80.8986	80.8986	77.1009	77.081
	5	77.6328	77.1109	77.1107	77.1106	77.1106		
	7	77.6230	77.1013	77.1010	77.1009	77.1009		
	9	77.6230	77.1012	77.1010	77.1009	77.1009		
	11	77.6230	77.1012	77.1010	77.1009	77.1009		
2	3	77.7587	77.2347	77.2344	77.2343	77.2343		
	5	77.6230	77.1013	77.1010	77.1010	77.1010		
3	3	77.6525	77.1302	77.1300	77.1299	77.1299		
	5	77.6230	77.1013	77.1010	77.1009	77. 1009		
4	3	77.6326	77.1107	77.1105	77.1104	77.1104		
6	3	77.6249	77.1032	77.1029	77.1029	77.1029		
8	3	77.6236	77.1019	77.1016	77.1015	77.1015		
12	3	77.6231	77.1014	77.1011	77.1011	77.1011		
16	3	77.6230	77.1013	77.1010	77.1010	77.1010		
20	3	77.6230	77.1013	77.1010	77.1009	77.1009		

Table 7
Convergence of buckling load (Na^2/D) of a SCSC isotropic square plate under uniaxial linearly varying compressive load ($\alpha = 0.25$)

n	*p*	*m*=9	*m*=11	*m*=13	*m*=15	*m*=17	Ref. [30]
1	3	98.6974	98.6902	98.6901	98.6901	98.6901	86.6689
	5	87.0105	86.9762	86.9754	86.9754	86.9754	
	7	86.7054	86.6712	86.6704	86.6704	86.6704	
	9	86.7040	86.6697	86.6689	86.6689	86.6689	
	11	86.7040	86.6697	86.6689	86.6689	86.6689	
	13	86.7040	86.6697	86.6689	86.6689	86.6689	
2	3	96.2247	96.1898	96.1890	96.1890	96.1890	
	5	86.7284	86.6942	86.6934	86.6934	86.6934	
	7	86.7040	86.6697	86.6690	86.6689	86.6689	
4	3	87.0366	87.0023	87.0015	87.0015	87.0015	
	5	86.7040	86.6698	86.6690	86.6690	86.6690	
5	3	86.8466	86.8124	86.8116	86.8116	86.8116	
	5	86.7040	86.6697	86.6689	86.6689	86.6689	
10	3	86.7135	86.6792	86.6785	86.6784	86.6784	
20	3	86.7046	86.6703	86.6695	86.6695	86.6695	
30	3	86.7041	86.6698	86.6691	86.6690	86.6690	
40	3	86.7040	86.6698	86.6690	86.6690	86.6690	
45	3	86.7040	86.6697	86.6690	86.6689	86.6689	

Table 8

Non-dimensional critical buckling loads (Na^2 / D) of SSSS isotropic rectangular plates under different linearly varying compressive loads (n = 1, p = 9, m = 16)

a/b	α = 0.8			α = 1			α = 2		
	Present	Ref. [30]	Ref. [46]	Present	Ref. [30]	Ref. [46]	Present	Ref. [30]	Ref. [46]
0.4	131.3579	131.3579	131.452	149.5357	149.5357	149.623	287.1940	287.1946	287.205
0.6	82.4374	82.4374	82.703	96.1641	96.1641	96.131	238.0719	238.0720	238.071
0.75	70.2014	70.2014	70.268	82.5896	82.5896	83.004	237.9742	237.9743	237.952
1	65.0906	65.0906	65.236	77.1009	77.1009	77.081	251.9547	251.9549	252.863
1.5	70.2014	70.2014	70.275	82.5896	82.5896	82.708	237.9742	237.9743	237.859

Table 9

Non-dimensional critical buckling loads (Na^2 / D) for SCSC isotropic rectangular plate under different linearly varying compressive loads (n = 1, p = 9, m = 16, a/b = 0.7)

α	Present	Ref. [30]	Ref. [46]	Ref. [47]	Ref. [48]
0	69.0952	69.0952	69.088	69.095	69.10
1	134.5895	134.5895	134.592	134.589	134.6
2	422.4652	422.4663	422.473	422.465	422.5

Table 10

Convergence of fundamental frequency ($\Omega_1 = \omega_1 a^2\sqrt{\rho h/D_{11}}$) of an orthotropic CCCC plate ($D_{33} = D_{22} = 1.5D_{11}$, n = 1)

a/b	*p*	*m*=9	*m*=11	*m*=13	*m*=15	*m*=17	Ref. [49]	Ref. [50]
1	5	41.1350	41.1333	41.1332	41.1332	41.1332	41.12	41.10
	7	41.1123	41.1098	41.1097	41.1097	41.1097		
	9	41.1081	41.1049	41.1047	41.1047	41.1047		
	11	41.1079	41.1044	41.1043	41.1043	41.1043		
	13	41.1079	41.1044	41.1043	41.1043	41.1043		
	15	41.1079	41.1044	41.1043	41.1043	41.1043		
0.5	5	25.6397	25.6368	25.6367	25.6367	25.6367	25.60	25.60
	7	25.6079	25.6055	25.6054	25.6054	25.6054		
	9	25.6072	25.6046	25.6046	25.6045	25.6045		
	11	25.6072	25.6046	25.6045	25.6045	25.6045		
	13	25.6072	25.6045	25.6045	25.6045	25.6045		
	15	25.6072	25.6045	25.6045	25.6045	25.6045		

Table 11

Convergence of fundamental frequency ($\Omega_1 = \omega_1 a^2\sqrt{\rho h/D_{33}}$) of an square orthotropic CCCC plate with initial stresses ($D_{11} = D_{22} = 2D_{33}$, $N_x = N_y = N$, n = 1)

N_0a^2/π^2D_{33}	p	m=9	m=11	m=13	m=15	Ref. [50]	Ref. [51]
-2	5	42.7131	42.7154	42.7154	42.7154	42.641	42.641
	7	42.6414	42.6428	42.6428	42.6428		
	9	42.6404	42.6414	42.6414	42.6414		
	11	42.6404	42.6414	42.6413	42.6413		
	13	42.6404	42.6414	42.6413	42.6413		
	15	42.6404	42.6414	42.6413	42.6413		
0	5	47.9823	47.9828	47.9828	47.9828	47.959	47.959
	7	47.9605	47.9603	47.9602	47.9602		
	9	47.9595	47.9590	47.9589	47.9589		
	11	47.9594	47.9589	47.9589	47.9589		
	13	47.9594	47.9589	47.9589	47.9589		
	15	47.9594	47.9589	47.9589	47.9589		
10	5	68.2723	68.2617	68.2615	68.2615	68.165	68.165
	7	68.1800	68.1694	68.1693	68.1692		
	9	68.1758	68.1652	68.1650	68.1650		
	11	68.1758	68.1652	68.1649	68.1649		
	13	68.1758	68.1651	68.1649	68.1649		
	15	68.1758	68.1651	68.1649	68.1649		
20	5	83.5830	83.5599	83.5590	83.5589	83.206	83.206
	7	83.2466	83.2236	83.2227	83.2227		
	9	83.2306	83.2076	83.2066	83.2066		
	11	83.2303	83.2073	83.2064	83.2064		
	13	83.2303	83.2073	83.2064	83.2064		
	15	83.2303	83.2073	83.2064	83.2064		

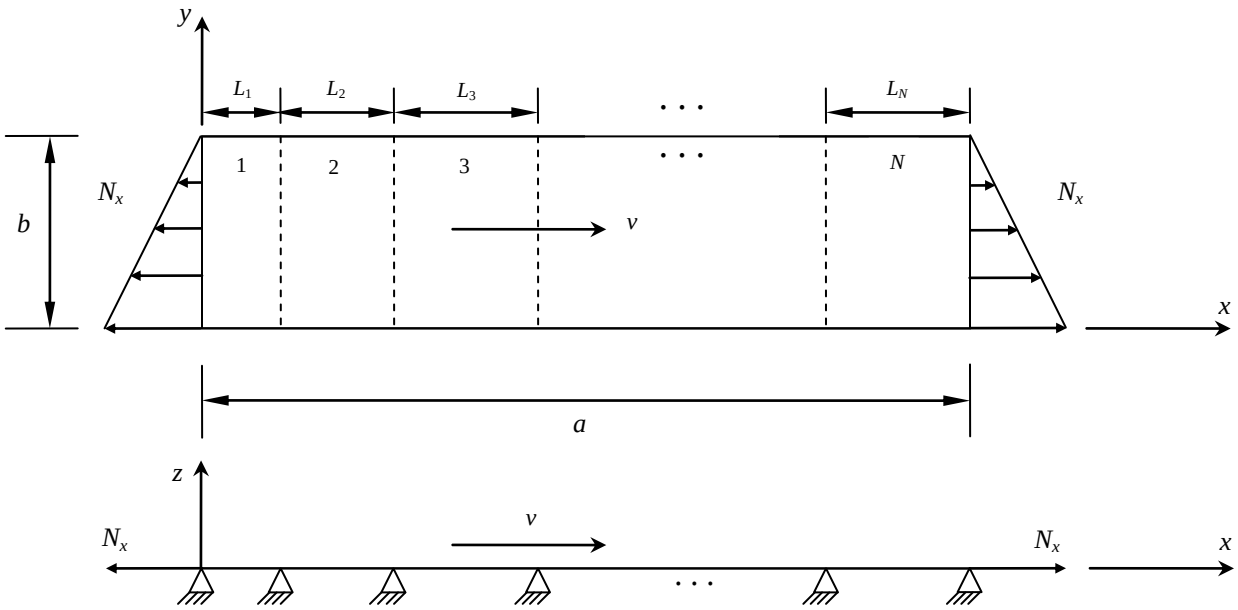

Fig. 1 Geometry and co-ordinate system for an axially moving orthotropic plate with (N – 1) internal line supports subjected to a non-uniform inplane axial force (tension).

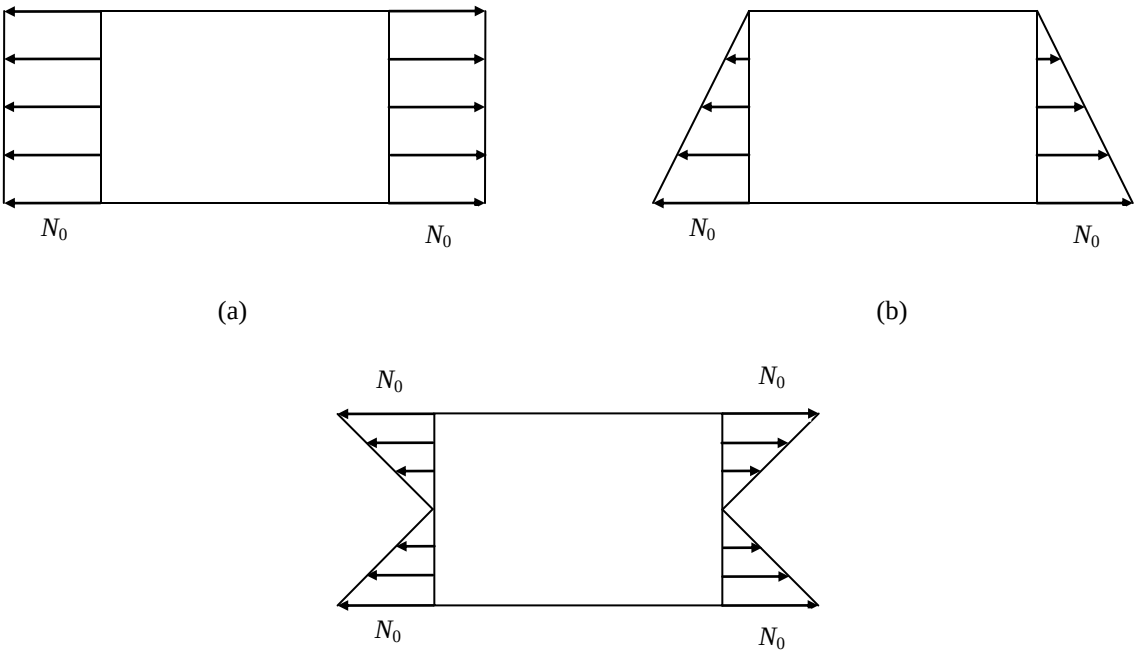

Fig. 2 A single span rectangular plate under different types of edge loading: (a) α = 0; (b) α = 1; (c) α = 2.

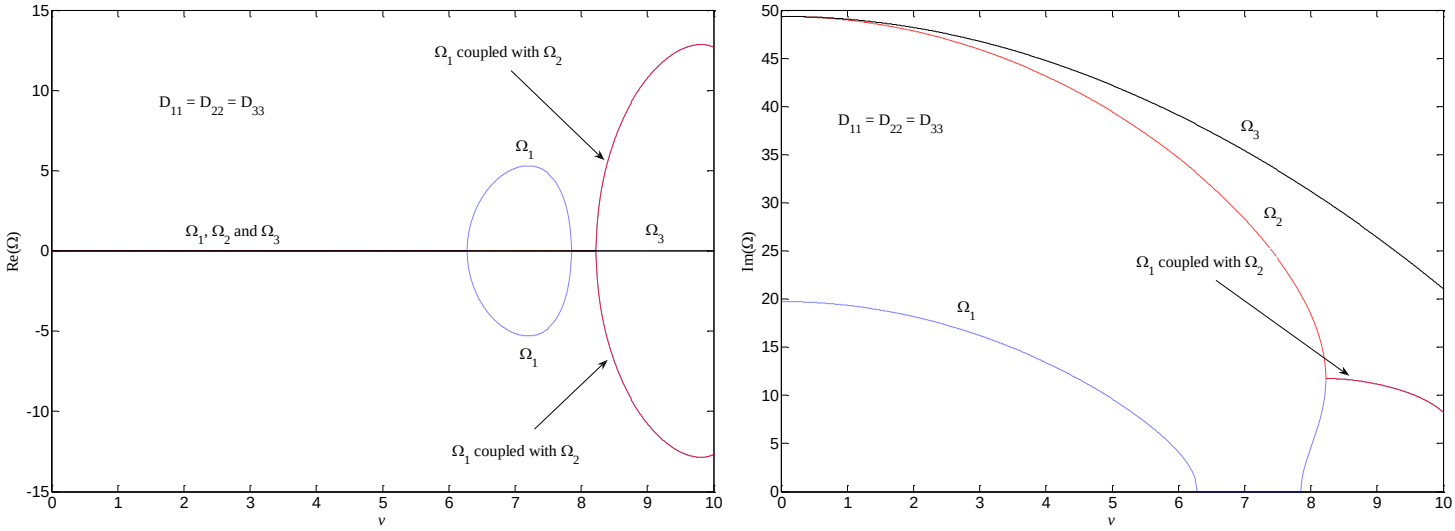

Fig. 3 Dimensionless complex frequencies of axially moving single-span isotropic SSSS square plates versus axially moving speed.

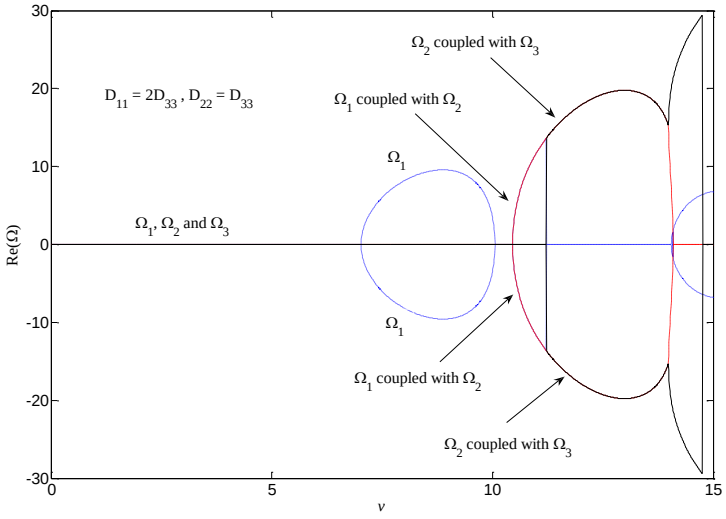
$D_{11} = 2D_{33}$, $D_{22} = D_{33}$
Ω_2 coupled with Ω_3
Ω_1 coupled with Ω_2
Ω_1
Ω_1, Ω_2 and Ω_3
Ω_1
Ω_1 coupled with Ω_2
Ω_2 coupled with Ω_3
Re(Ω)
ν

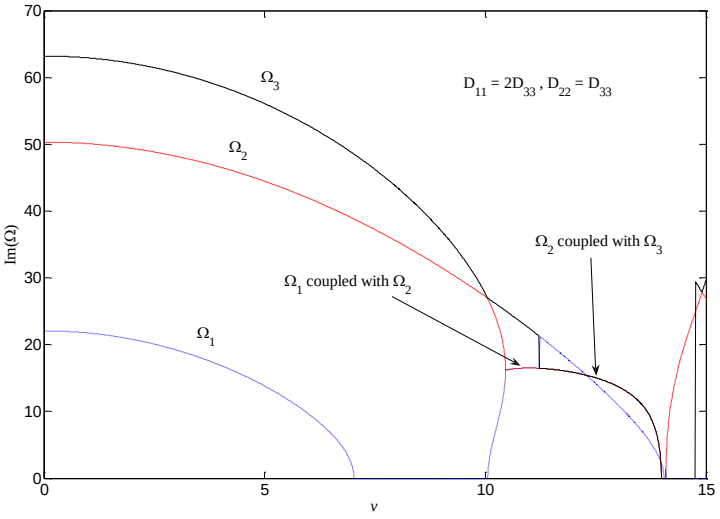
$D_{11} = 2D_{33}$, $D_{22} = D_{33}$
Ω_3
Ω_2
Ω_2 coupled with Ω_3
Ω_1 coupled with Ω_2
Ω_1
Im(Ω)
ν

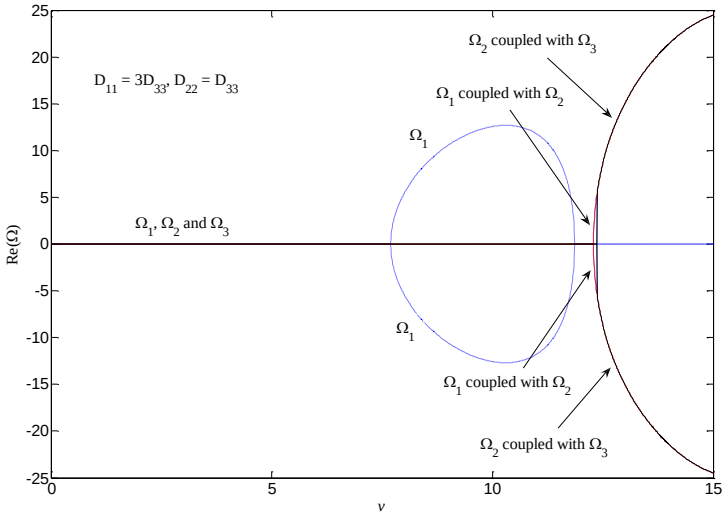
$D_{11} = 3D_{33}$, $D_{22} = D_{33}$
Ω_2 coupled with Ω_3
Ω_1 coupled with Ω_2
Ω_1
Ω_1, Ω_2 and Ω_3
Ω_1
Ω_1 coupled with Ω_2
Ω_2 coupled with Ω_3
Re(Ω)
ν

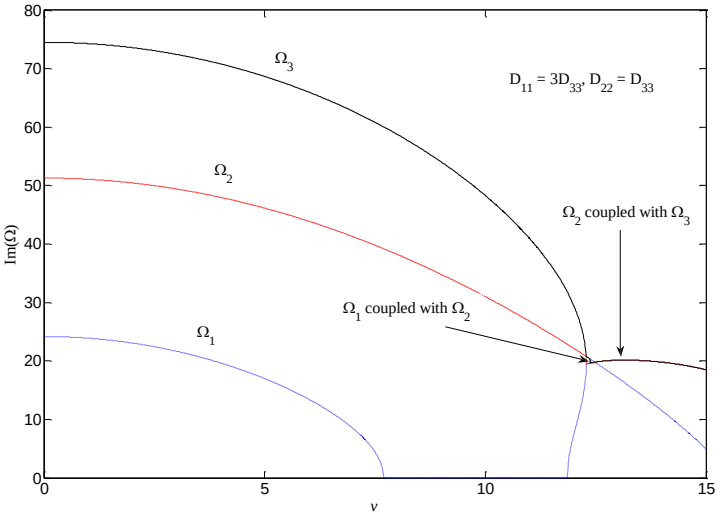
$D_{11} = 3D_{33}$, $D_{22} = D_{33}$
Ω_3
Ω_2
Ω_2 coupled with Ω_3
Ω_1 coupled with Ω_2
Ω_1
Im(Ω)
ν

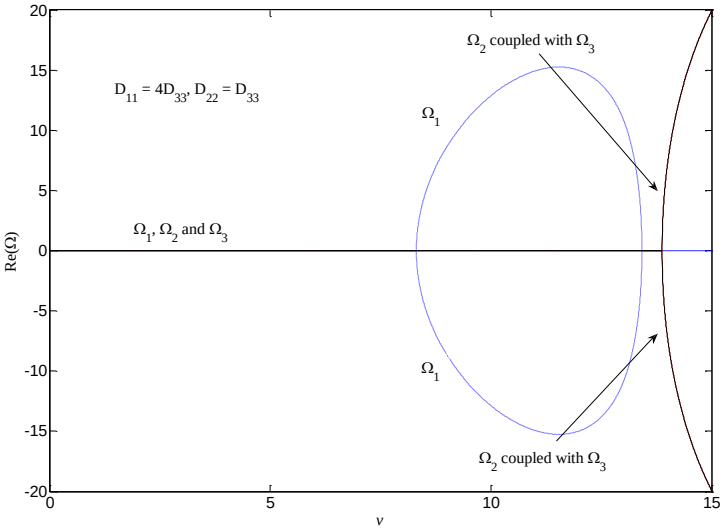
$D_{11} = 4D_{33}$, $D_{22} = D_{33}$
Ω_2 coupled with Ω_3
Ω_1
Ω_1, Ω_2 and Ω_3
Ω_1
Ω_2 coupled with Ω_3
Re(Ω)
ν

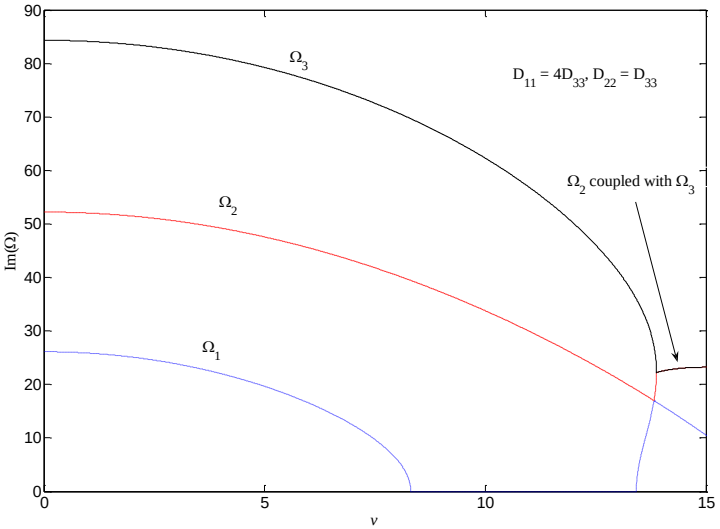
$D_{11} = 4D_{33}$, $D_{22} = D_{33}$
Ω_3
Ω_2
Ω_2 coupled with Ω_3
Ω_1
Im(Ω)
ν

Fig. 4 Dimensionless complex frequencies of axially moving single-span orthotropic SSSS square plates versus axially moving speed for different values of D_{11}.

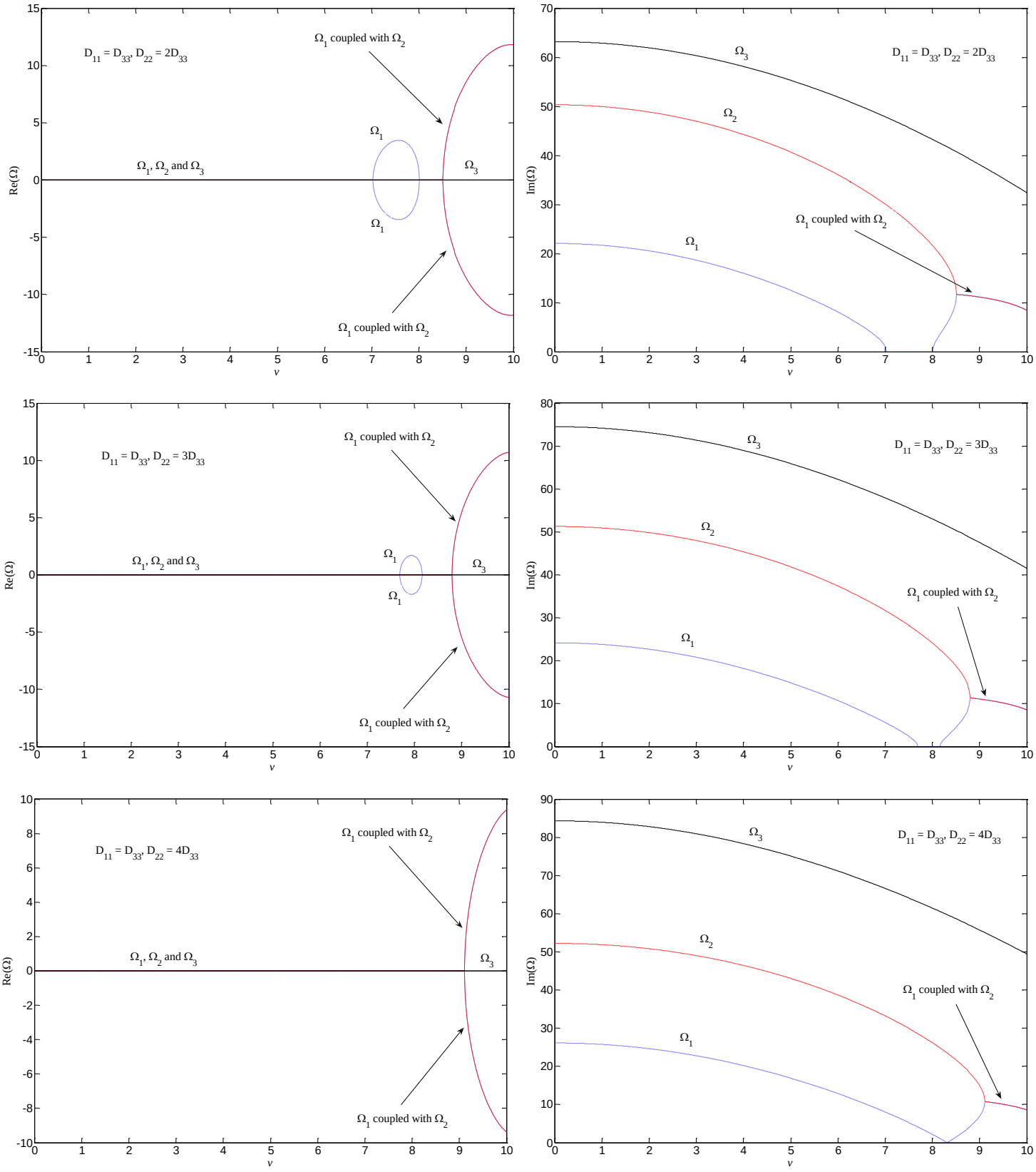

Fig. 5 Dimensionless complex frequencies of axially moving single-span orthotropic SSSS square plates versus axially moving speed for different values of D_{22}.

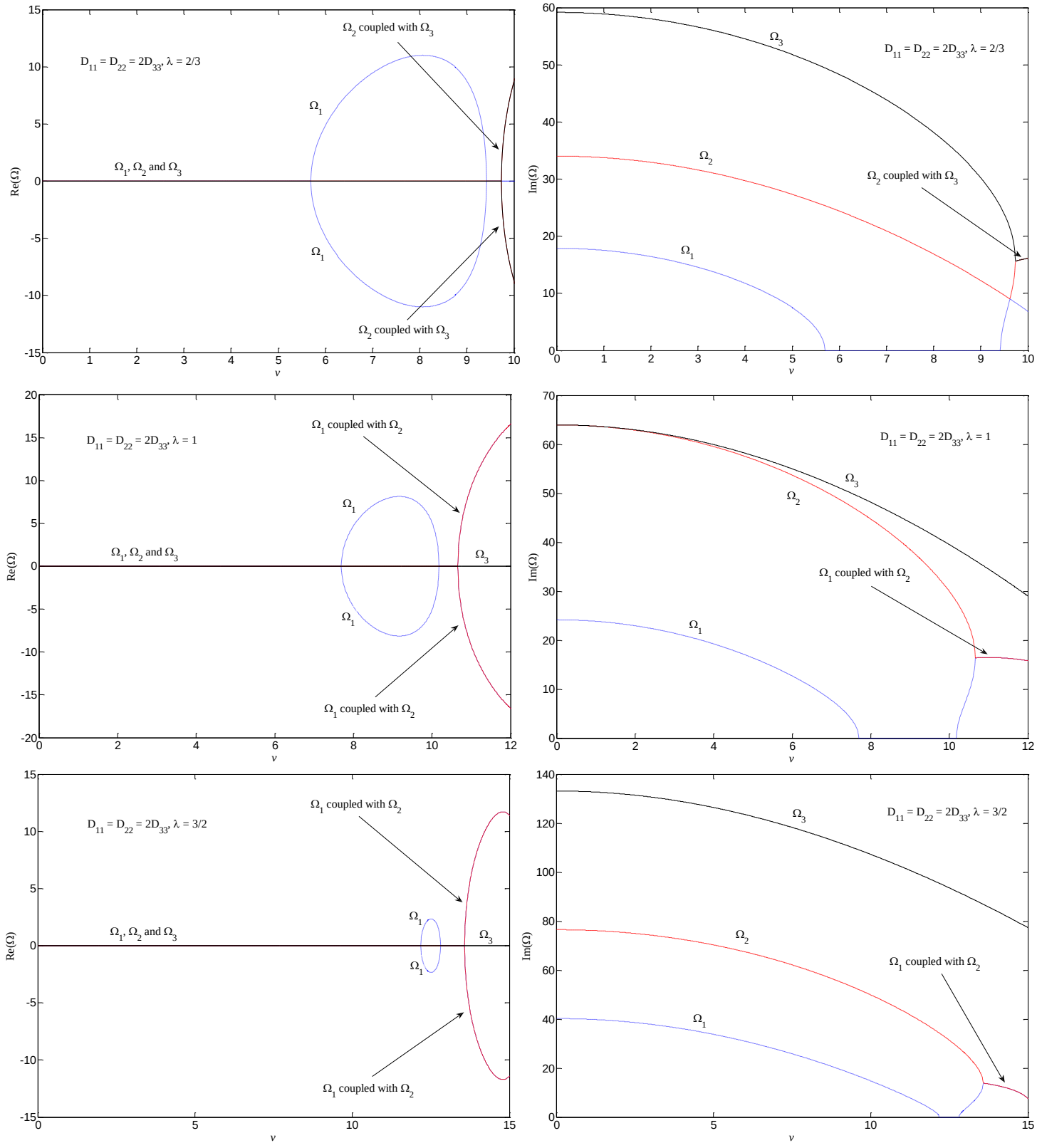

Fig. 6 Dimensionless complex frequencies of axially moving single-span orthotropic SSSS rectangular plates versus axially moving speed for different values of $\lambda = a/b$.

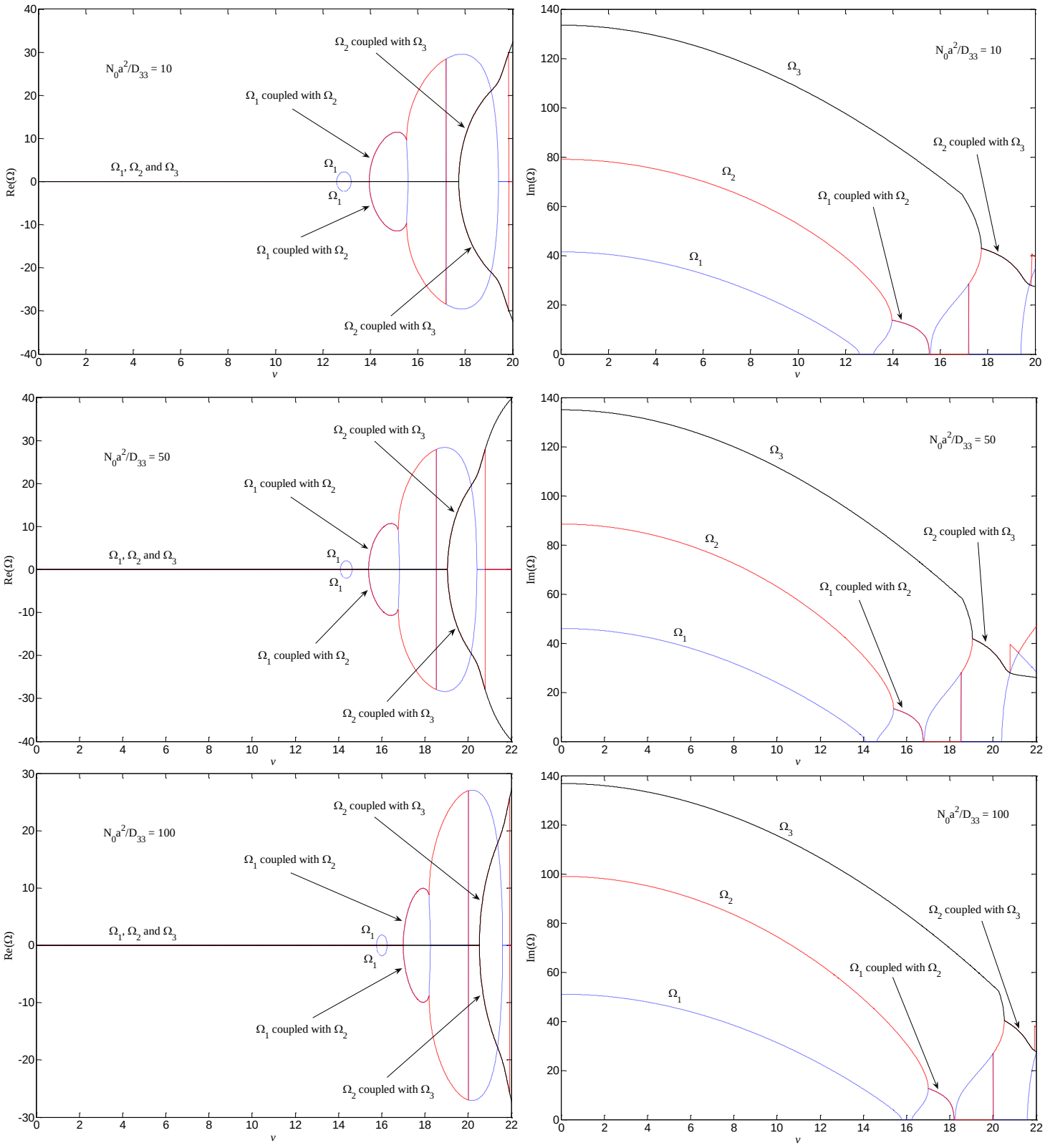

Fig.7 Dimensionless complex frequencies of axially moving single-span orthotropic SSSS rectangular plates versus axially moving speed for different values of inplane forces ($D_{11} = D_{22} = 2D_{33}$, $\lambda = 3/2$, $\alpha = 0$).

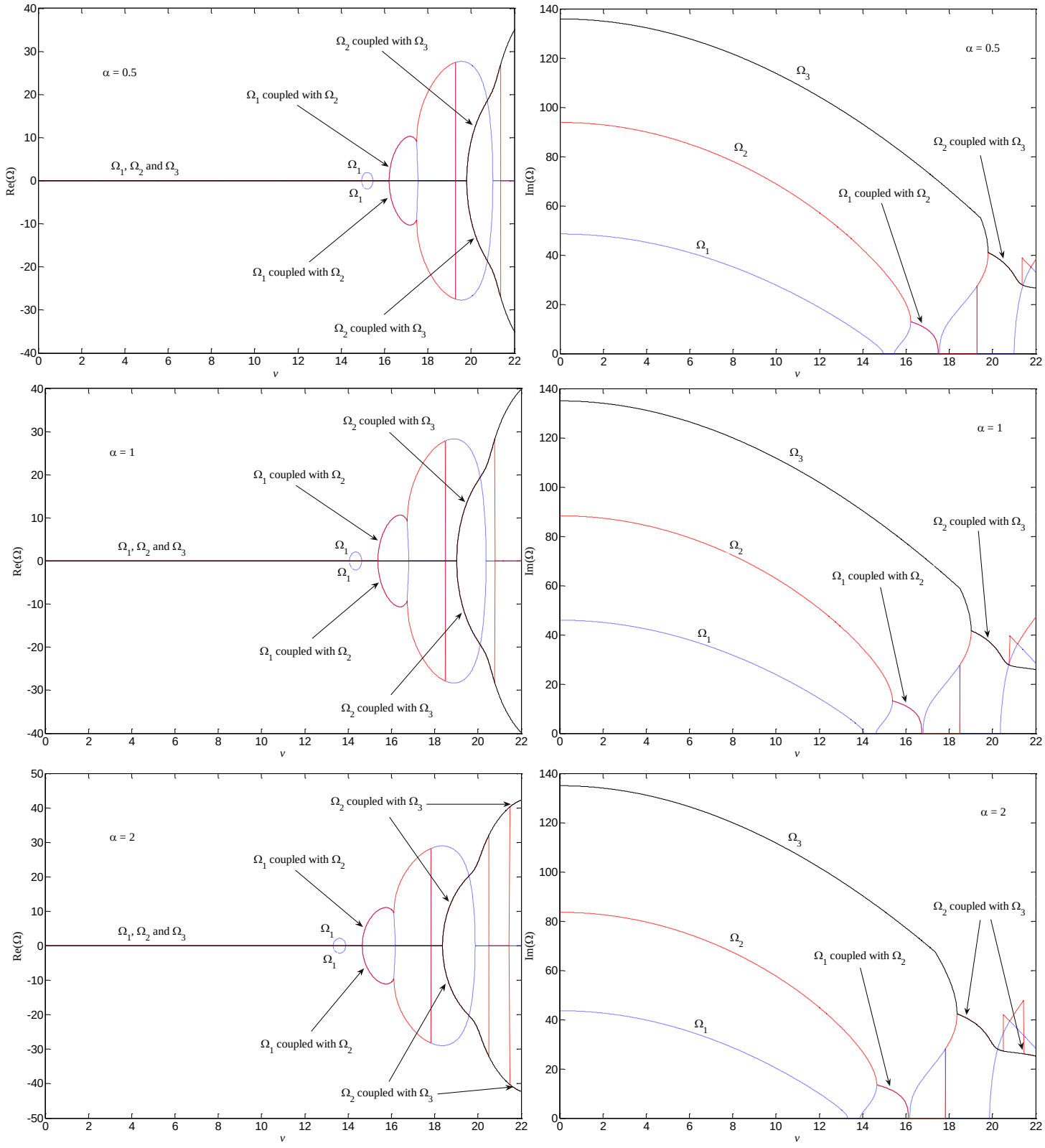

Fig.8 Dimensionless complex frequencies of axially moving single-span orthotropic SSSS rectangular plates versus axially moving speed for different values of α ($D_{11} = D_{22} = 2D_{33}$, λ = 3/2, $N_0a^2/D_{33} = 100$).

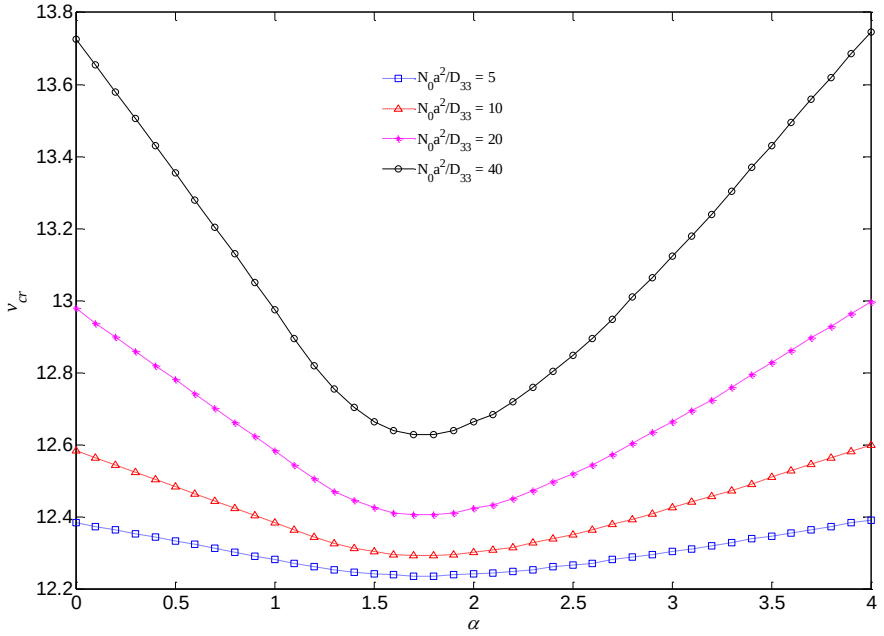

Fig.9 Variation of critical velocity of an axially moving single-span orthotropic SSSS rectangular plates versus α-value for different values of N_0 ($D_{11} = D_{22} = 2D_{33}$, $\lambda = 3/2$).

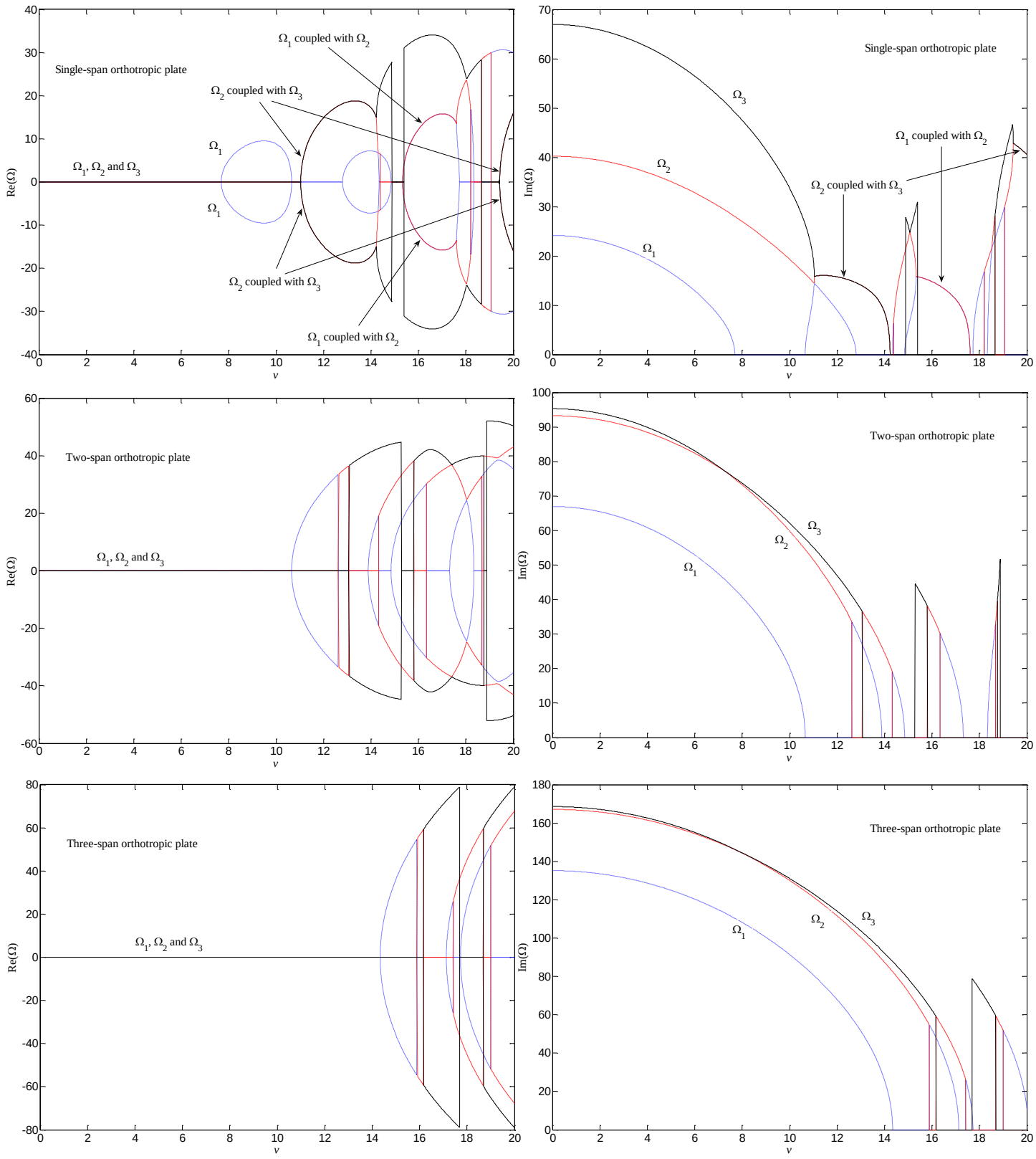

Fig.10 Dimensionless complex frequencies of axially moving multi-span orthotropic SFSF rectangular plates versus axially moving speed ($D_{11} = D_{22} = 2D_{33}$, $\lambda = 3$, $N_0\alpha^2/D_{33} = 100$, $\alpha = 1$).